AD-A157 714

FINAL REPORT ON INVESTIGATION OF ALCOHOL COMBUSTION ASSOCIATED WEAR IN SPARK IGNITION ENGINES
Mechanisms and Lubricant Effects

INTERIM REPORT
AFLRL No. 176 ✓

By

D.W. Naegeli
E.C. Owens
U.S. Army Fuels and Lubricants Research Laboratory
Southwest Research Institute
San Antonio, Texas

Under Contract to

U.S. Army Belvoir Research and Development Center
Materials, Fuels, and Lubricants Laboratory
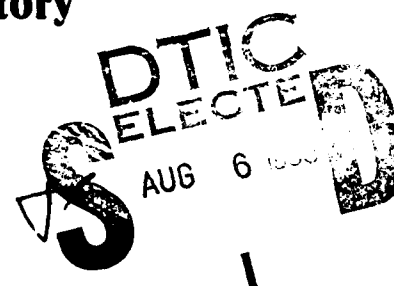**Fort Belvoir, Virginia**

Contract No. DAAK70-85-C-0007

and

U.S. Department of Energy
Heavy Duty Transport and Fuels Integration Branch
Washington, DC

Interagency Agreement No. DE-AI01-79CS50030

December 1984

85 · 7 30 051

DTIC FILE COPY

Disclaimers

The findings in this report are not to be construed as an official Department of the Army position unless so designated by other authorized documents.

Trade names cited in this report do not constitute an official endorsement or approval of the use of such commercial hardware or software.

DTIC Availability Notice

Qualified requestors may obtain copies of this report from the Defense Technical Information Center, Cameron Station, Alexandria, Virginia 22314.

Disposition Instructions

Destroy this report when no longer needed. Do not return it to the originator.

AD-A157714

REPORT DOCUMENTATION PAGE

1a. REPORT SECURITY CLASSIFICATION	1b. RESTRICTIVE MARKINGS
Unclassified	None

2a. SECURITY CLASSIFICATION AUTHORITY	3. DISTRIBUTION/AVAILABILITY OF REPORT
	Approved for public release; distribution unlimited
2b. DECLASSIFICATION/DOWNGRADING SCHEDULE	

4. PERFORMING ORGANIZATION REPORT NUMBER(S)	5. MONITORING ORGANIZATION REPORT NUMBER(S)
Interim Report AFLRL No. 176	

6a. NAME OF PERFORMING ORGANIZATION	6b. OFFICE SYMBOL (If applicable)	7a. NAME OF MONITORING ORGANIZATION
U.S. Army Fuels and Lubricants Research Laboratory		

6c. ADDRESS (City, State, and ZIP Code)	7b. ADDRESS (City, State, and ZIP Code)
Southwest Research Institute 6220 Culebra Road San Antonio, TX 78284	

8a. NAME OF FUNDING/SPONSORING ORGANIZATION	8b. OFFICE SYMBOL (If applicable)	9. PROCUREMENT INSTRUMENT IDENTIFICATION NUMBER
Belvoir R&D Center	STRBE-VF	DAAK70-78-C-0001,WD5; DAAK70-80-C-0001,WD6 DAAK70-85-C-0007,WD27;DAAK70-82-C-0001,WD11 DAAK70-79-C-0175; IA No. DE-AI01-79C550030

8c. ADDRESS (City, State, and ZIP Code)	10. SOURCE OF FUNDING NUMBERS			
	PROGRAM ELEMENT NO.	PROJECT NO.	TASK NO.	WORK UNIT ACCESSION NO.
Fort Belvoir, Virginia 22060-5606				

11. TITLE (Include Security Classification)

Final Report on Investigation of Alcohol Combustion Associated Wear in Spark-Ignition Engines

12. PERSONAL AUTHOR(S)
Naegeli, David N. and Owens, Edwin C.

13a. TYPE OF REPORT	13b. TIME COVERED	14. DATE OF REPORT (Year, Month, Day)	15. PAGE COUNT
Interim	FROM Sep 1976 TO Dec 1984	1984 December	87

16. SUPPLEMENTARY NOTATION
This work provides final report requirements for "Engine Lubricants for Methanol-Fueled Vehicles" conducted under Contract Nos. DAAK70-78-C-0001 and KAAK70-79-C-0175 and for "Reactivity of Metals in Alcohol Fuel-Wetted Systems," conducted under Contract No. (over)

17.	COSATI CODES		18. SUBJECT TERMS (Continue on reverse if necessary and identify by block number)
FIELD	GROUP	SUB-GROUP	alcohol methanol ethanol corrosion, formaldehyde lubrication, engines formic- combustion, additives, gasohol acid.

19. ABSTRACT (Continue on reverse if necessary and identify by block number)

An investigation of the effects of alcohol fuels on spark ignition engine wear and deposition was jointly sponsored by the U.S. Department of Energy and the U.S. Army Belvoir Research and Development Center. This research has investigated four alcohol-containing fuels: pure methanol, pure ethanol, methanol in unleaded gasoline, and ethanol in unleaded gasoline (gasohol). Tests were conducted using a variety of single-cylinder research engines and production multicylinder engines, mounted in dynamometer test stands.

This testing indicated that pure alcohol fuels reduced the buildup of engine deposits. Also, neat methanol greatly increased engine wear rates at engine temperatures below 75°C, while anhydrous ethanol and the alcohol-gasoline blends did not increase wear rates over that of unleaded gasoline.

20. DISTRIBUTION/AVAILABILITY OF ABSTRACT	21. ABSTRACT SECURITY CLASSIFICATION
☐ UNCLASSIFIED/UNLIMITED ☒ SAME AS RPT. ☐ DTIC USERS	Unclassified

22a. NAME OF RESPONSIBLE INDIVIDUAL	22b. TELEPHONE (Include Area Code)	22c. OFFICE SYMBOL
Mr. F.W. Schaekel	(703) 664-3576	STRBE-VF

DD FORM 1473, 84 MAR   83 APR edition may be used until exhausted.   SECURITY CLASSIFICATION OF THIS PAGE
                                 All other editions are obsolete.

11. (Cont'd) Combustion Associated Wear in Spark Ignition Engines

16. (Cont'd) DAAK70-80-C-0001. This work was jointly funded by the Department of Energy Heavy Duty Transport and Fuels Integration Branch, through Interagency Agreement No. DE-AI01-79C550030, and Belvoir R&D Center.

18. (Cont'd) wettability
    iron formate

19. ABSTRACT (Cont'd)

Engine-based tests were conducted to investigate the effects of variations in lubricant base stocks and additive formulations on the wear observed with methanol. As part of this effort, a 20-hour steady-state test was developed for use in lubricant development. The study identified one lubricant formulation that was superior in controlling methanol-related cylinder bore wear, but still not to acceptable levels.

The mechanisms leading to this excessive wear with methanol were investigated using both engine and bench experiments. Engine tests indicated that the wear results from reactions between methanol combustion products and the cast-iron cylinder liner, where the presence of liquid methanol in the combustion chamber appears to be an important part of the mechanism. Bench experiments indicated that the presence of liquid methanol may interfere with the formation of lubricant films on the cylinder walls.

To determine interaction between fuel alcohols and engine metals, two approaches were developed. One approach uses an LFW-1 wear test machine with methanol applied to the wear area. The second approach employs hand lapping of alloy specimens with a slurry of fine abrasive and oil or abrasive with methanol. Electron spectroscopy for chemical analysis (ESCA) testing revealed a much higher oxygen content in the surface reaction product of samples prepared with methanol. The surface reaction product of the methanol-lapped specimens had a slight blue coloration and, when tested for surface wettability by measurement of the spread rate for an oil drop placed on the reacted surface, showed a reduction in spread rate as compared to samples prepared with oil lapping.

The role of nitrogen in this wear process was studied by operating a 2.3-liter engine fueled with methanol in a nitrogen-free atmosphere. The 20-hour steady-state test was carried out using a mixture of oxygen, argon, and carbon dioxide in place of air. The test showed that the wear as indicated by iron wear particle buildup in the oil was the same in the nitrogen-free test as that in baseline tests combusting methanol-air mixtures. It was concluded that nitric acid does not play a role in the corrosion of the upper cylinder bore and ring areas of methanol-fueled engines.

Bench experiments indicated that formicacid and peroxides are formed as methanol combustion intermediates. Further studies indicated that these materials diffuse into the liquid methanol layer on the cylinder wall and react rapidly with iron in the liner. The resulting iron formate decompose to iron oxide and is then removed from the liner by the action of the piston rings. The results from these bench experiments were confirmed through sampling of the quench layers of engines operating on methanol.

Originator supplied Keywords

FOREWORD

The work reported herein was conducted at the U.S. Army Fuels and Lubricants Research Laboratory (AFLRL), Southwest Research Institute, San Antonio, TX, under Contract Nos. DAAK70-78-C-0001, DAAK70-79-C-0175, DAAK70-80-C-0001, DAAK70-82-C-0001, and DAAK70-85-C-0007 and Department of Energy Interagency Agreement No. DE-AI01-79CS50030 and covers the period September 1976 - December 1984. The work was jointly funded by the U.S. Army Belvoir Research and Development Center (STRBE-VF), Ft. Belvoir, VA, and the U.S. Department of Energy, Heavy Duty Transport and Fuels Integration Branch (HDTFIB), Wash-<ington, D.C. Contract Officer's representative was Mr. F.W. Schaekel, Materials, Fuels, and Lubricants Laboratory/STRBE-VF, and the technical monitors for the Department of Energy were Mr. E.E. Ecklund, Chief, HDTFIB, and Mr. G. Prok, NASA/Lewis, Cleveland, OH.

TABLE OF CONTENTS

3

LIST OF ILLUSTRATIONS

LIST OF TABLES

I. INTRODUCTION

With the decline of the petroleum era in sight, it has become necessary to develop alternative fuels from more abundant energy sources such as coal and natural gas. This necessity has sparked a renewed interest in alcohols. Alcohols were used to fuel automobiles early in the century until the lower price of gasoline removed them from the market. Recent studies have shown that alcohols, namely methanol, not only provide an alternative for gasoline in the U.S., but also may well improve the thermodynamic efficiency and performance; as well as reduce the cost of catalytic emission control devices for spark ignition engines. On the other hand, research has also shown that alcohol fuels have several problems, including cold start ignition, fuel system corrosion, elastomer incompatibility, explosive vapor space in fuel tank, and abnormally high upper cylinder bore and ring wear. The latter, which is discussed in this report, has been observed by several workers (1-6)* in both laboratory engine studies and vehicle fleet tests. The increased cylinder bore and ring wear is most pronounced during low-temperature engine operation and is expected to be particularly troublesome in cooler climates.

This report reviews the work done at AFLRL in identifying the conditions under which increased wear occurs with methanol and AFLRL efforts in selecting promising lubrication approaches to alleviating this wear problem. Also reported here are investigations into the underlying mechanisms responsible for the increased wear.

II. BACKGROUND

While alcohols--methanol and ethanol in particular--have been considered for and sometimes used as automotive fuels almost since the beginning of the automobile, usage has generally been restricted to periods of emergency or racing. In these applications, little attention has been given to alcohol

---

* Underscored numbers in parentheses refer to the list of references at the end of this report.

effects on engine wear and deposits. While general references have been made to increased wear, only a few quantitative results have been reported in the literature, and the majority date into the 1930's.(7-9) Obviously, engine metallurgy and particularly oil formulations have changed considerably in the past 50 years. However, the same wear-inducing processes are involved in the combustion of alcohol in current engines. Incomplete combustion products of alcohol found in the blowby gases contaminating the engine oil sump contain organic acids and aldehydes which can increase corrosion, particularly under conditions of moisture condensation. Additionally, since alcohol contained in the blowby gases is polar, it would be expected to react with many of the lubricant additives and thus interfere with the inhibitors normally available to control engine deposits and wear.

The current interest in methanol and higher alcohols is for their use as a replacement for petroleum-derived fuel supplies. Therefore, the lubricant-related problems which had been ignored or tolerated in periods of dire necessity must now be addressed and solved before alcohol can be considered a practical fuel for general consumer usage. During the past several years, as alcohol has again become a serious contender as an alternate automotive fuel in the United States, some initial studies of the effects of alcohol-containing fuels on engine lubrication have been undertaken.

A brief study by Continental Oil Company which experienced excessive wear problems with pure methanol fuels during conduct of an ASTM Sequence V-C test procedure was one of the first items of hard data indicating that a compati-bility problem may exist with alcohol fuels with current engines and lubri-cants.(10) Partially as a result of this initial data, the work reported herein was funded by the United States Department of Energy to ascertain the effects of alcohols, particularly methanol, on wear- and lubricant-related deposit formation, and if problems exist, to aid the development of lubricant additives or lubricant formulations to control these deleterious effects.

The investigation of the effects of alcohol fuels on the oil-wetted portions of an engine was started using a single-cylinder Coordinating Lubricants Research (CLR) engine fueled with pure (Technical grade) methanol. Based on

8

the Conoco work and as a result of a limited amount of radioactive tracer work (1) the initial investigations concentrated on low engine temperature operations. A series of CLR engine tests indicated that the use of pure methanol greatly increased the rate at which iron wear particles accumulated in the engine oil.(11) Because the CLR engine is significantly different from current engine designs and to confirm these initial results in a full-scale modern engine, a test stand capable of conducting the ASTM Sequence V-D (12) test was set up. The engine used was a 2.3-liter Ford overhead cam four-cylinder design and was set up in accordance with the V-D procedures, except that all engine blocks were bored 0.51 mm oversize and fitted with appropriate pistons. The overbored blocks were obtained from the SwRI oil testing division. These blocks would normally have been used for fourth-build sequence V-D engines. Their use in this program not only provided for a consistent bore size and finish but also reduced the project costs. The entire engine, except for the plated oil pan and rocker cover, was discarded at the conclusion of each test.

The engine test was found to be reasonably repeatable in evaluating wear as indicated by subsequent oil analysis which measured the level of wear metals accumulated in the oil. The wear rate with pure methanol and a commercially available MIL-L-46152 product (Lubricant A) appeared to be reasonably repeat-able, but at a much higher level of iron wear metals than with unleaded gasoline. The difference in wear rates between pure methanol and Phillips J unleaded gasoline as indicated by iron wear metal accumulation is illustrated graphically in Figure 1. When corrected for oil consumption differences, the average iron wear rate with methanol was 18.9 mg/hr, 5.9 times the 3.2 mg/hr rate with Phillips J unleaded gasoline. Other differences in engine wear measurements and deposit levels are shown in Table 1. In general, the increased wear appeared to be primarily in the piston ring and cylinder bore area with the remainder of the engine unaffected. As expected, the engine varnish deposits were reduced.

Used oil analyses, Table 2, showed no significant differences between the methanol and Phillips J fueled tests other than the wear metals and water content. With Lubricant A, the final drain with methanol had almost eight

9
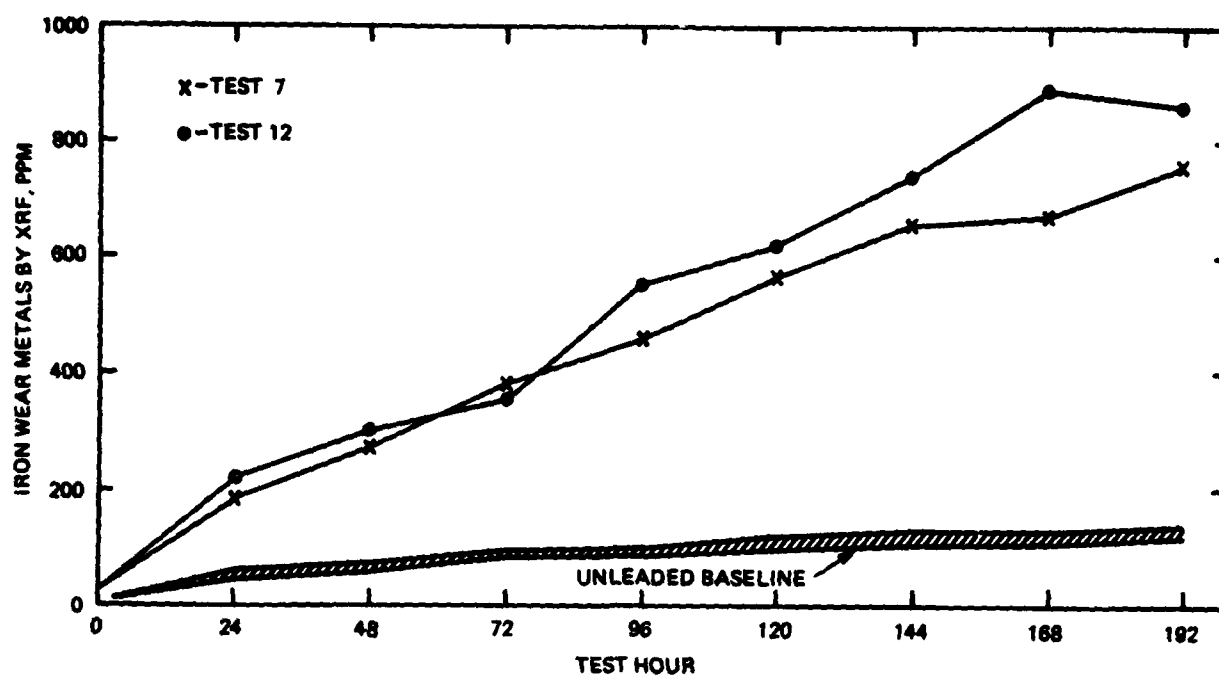
FIGURE 1. WEAR METAL ACCUMULATION RATE WITH
PURE METHANOL AND LUBRICANT A

TABLE 1. POST-TEST INSPECTIONS -- METHANOL AND LUBRICANT A

Test No.	7	12	Avg. Three-Test Baseline
Fuel	Methanol	Methanol	Phillips J
Lubricant	A	A	A
Duration, hr	192	192	192
Avg Sludge Deposits*	9.73	9.73	9.80
Piston Skirt Varnish*	9.91	9.93	7.91
Avg Varnish Deposits*	9.50	9.83	8.63
Top Ring Gap Incr, mils, max	13.0	9.0	3.3
Top Ring Gap Incr, mils, avg	7.0	6.0	1.8
Rod Brg, Wt Loss, mg, max	72.4	46.5	37.5
Rod Brg, Wt Loss, mg, avg	45.9	35.7	32.7
Cam Follower, Wt Loss, mg, max	9.8	537.5	2.5
Cam Follower, Wt Loss, mg, avg	4.3	116.4	1.7
Cam Lobe Wear, mils, max	1.4	16.9	0.57
Cam Lobe Wear, mils, avg	1.2	4.2	0.37

*10 = Clean

10

TABLE 2.   USED OIL ANALYSES

Lubricant	FREO-200-3	FREO-200-3	A*	A*
Fuel	Methanol	Phillips J	Methanol	Phillips J
Properties				
K Vis, cSt				
at 40°C	53.6	42.3	63.9	57.3
at 100°C	ND	7.4	10.3	9.3
Flash Point, °C	ND	140	183	154
Total Acid No.	ND	7.4	3.8	4.2
Total Base No. (D 664)	ND	0.3	2.3	2.0
Insolubles, w/coag				
Pentane, wt%	ND	0.46	0.36	0.30
Toluene, wt%	ND	0.17	0.22	0.14
Wear Metals, ppm by AA				
Fe	5850	154	815	102
Cu	104	9	26	10
Cr	79	1	8	2
Pb	213	27	64	53
Water Content, wt%	ND	0.11	0.51	0.24

ND = Not determined.
* = Avg of two tests.

times as much iron and at least twice as much copper as the engine fueled with Phillips J unleaded gasoline. This indicates that the increased wear observed with methanol is occurring without permanently altering the bulk oil properties.

Microscopic examination of the piston rings from the CLR engine tests, Figure 2, indicated that corrosive attack played some part in the increased wear in that engine. The photographs show a section of the cast-iron piston rings magnified 32 and 400 times. In the right photograph, the bright surface is that part of the ring which contacts the cylinder wall and is polished through normal wear. This same surface in the left-hand picture shows that this wear surface appears to be lightly etched as if prepared for a metallurgical examination. The greater width of this area indicates the greater amount of wear of the ring. It was, therefore, concluded that corrosive attack was taking place. However, only the rubbing surfaces showed evidence of corrosive action so it appears that the corrosive agent required a fresh metal surface. This may indicate that the corrosive agent is a weaker acid that would not react with the metal-oxide film present in the noncontact areas.
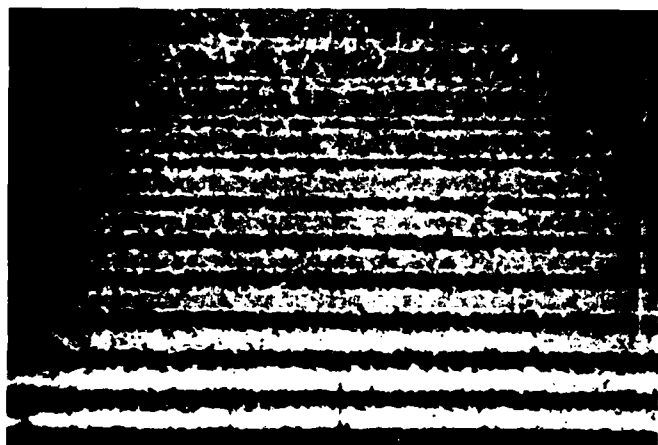
32X Magnification
(Reduced 12% in reproduction)
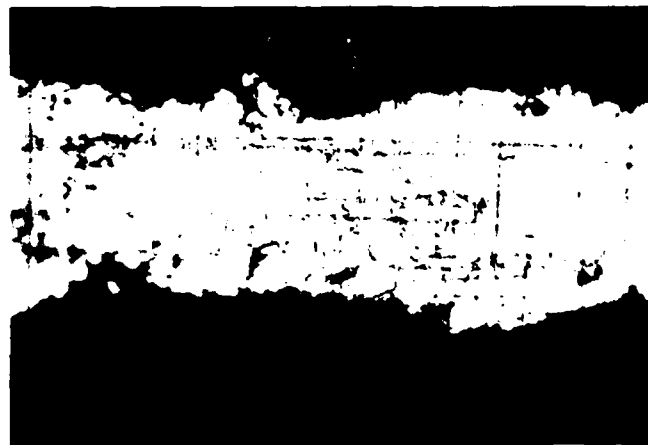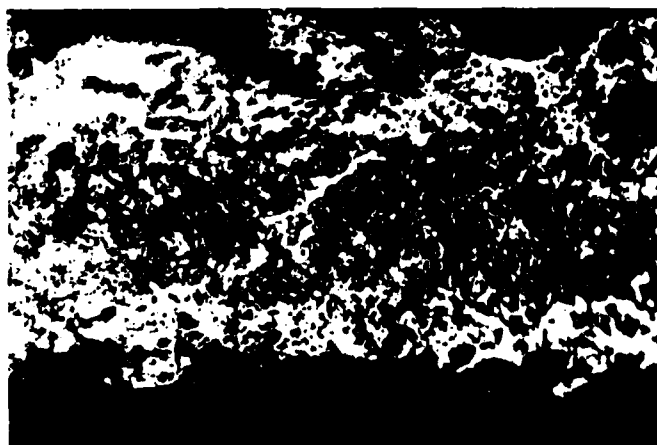
400X Magnification
(Reduced 12% in reproduction)

METHANOL   UNLEADED GASOLINE

FIGURE 2.   MICROSCOPIC EXAMINATION OF CAST-IRON RING FACE

A. 2.3-Liter Engine 20-Hour Steady-State Test

Tests were conducted with the multicylinder 2.3-liter engine to determine the effects of engine operating temperature on wear metal generation with various fuels. Lubricant A was used for this entire study. The fuels examined were neat anhydrous methanol, methanol containing 11 percent deionized water, anhydrous ethanol, ethanol with 11 percent deionized water, and Phillips J unleaded gasoline.

It appears that all the fuels had approximately the same wear metal generation rates until the oil sump temperature was lowered below 70°-80°C. Below this temperature range, the wear metal production increased rapidly, as illustrated in Figure 3. In this figure, the shaded region bounds an eight-test band generated using eight different batches of anhydrous methanol. The anhydrous methanol data contrast sharply with the anhydrous ethanol and the gasoline results depicted by the dashed line.

While this result with methanol confirmed the modified sequence V-D results, AFLRL results with ethanol conflicted with increased wear results reported by other researchers using "wet" ethanol. As a result, 11 percent water was added to both alcohol fuels, and these "wet" fuels were evaluated using this procedure, again holding the equivalence ratio constant. Tests conducted with "wet" ethanol fuel showed increased wear resulting from the water addition. For example, at 46°C oil-in temperature, this fuel produced 52 ppm of iron compared to 12 ppm iron wear metals with the anhydrous ethanol. The same type of wear increase was observed with the methanol containing water, where the water addition increased iron wear metal production by about 300 percent over that observed with the anhydrous methanol at temperatures below the 70°-80°C threshold.

1. Fully Formulated Lubricants

With the establishment of a test procedure that appeared to distinguish between neat methanol fuel and unleaded gasoline in terms of wear with Lubricant A, the next activity concentrated on evaluating various lubricant formu-
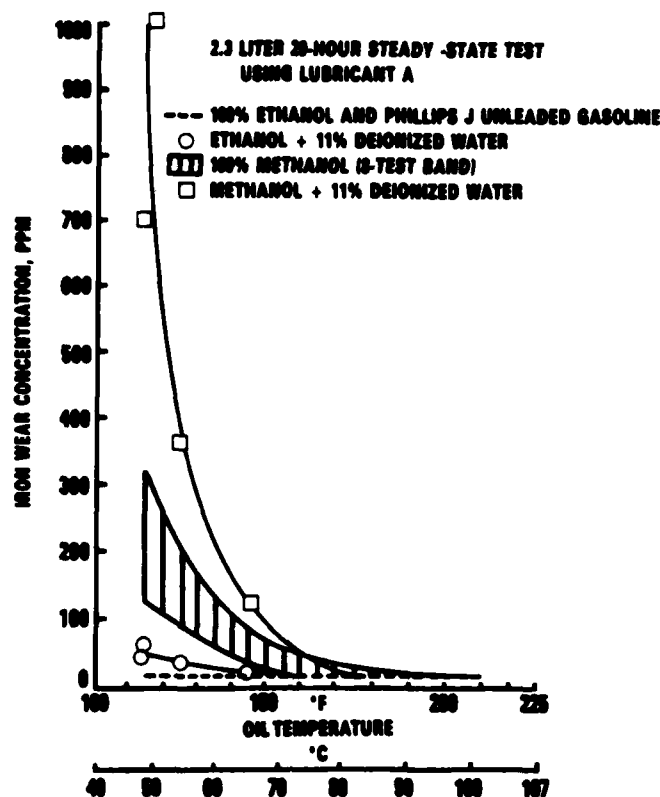
FIGURE 3. EFFECT OF OIL SUMP TEMPERATURE ON
ENGINE IRON WEAR WITH VARIOUS FUELS

lations. Several lubricants, some of which had shown positive results in the single-cylinder CLR engine, were obtained. These lubricants' characteristics are listed in Table 3. The modified Sequence V-D test was conducted with these lubricants using pure methanol as fuel. Lubricants B, C, D, E, and G were selected because of their good performances when screened in the CLR single-cylinder engine. Lubricants B, C, D, and E had less iron concentration than did Lubricant A, while Lubricant G had the same iron concentration as Lubricant A in the CLR single-cylinder engine.(1)

In summary, none of the ten lubricants evaluated using neat methanol fuel exceeded the performance of Lubricant A. However, Lubricant A performance with methanol fuel still would not be adequate for low-temperature operation. The results also appear to show that the CLR single-cylinder engine and the

14

TABLE 3. NEW LUBRICANT PROPERTIES

Oil Code	ASTM Test Method	A	B	C	D	E	F	G	H	I	J	K
40°C, cSt	D 445	68.9	65.4	106.0	26.3	71.8	97.0	56.0	30.1	96.1	125.9	77.4
100°C, cSt	D 445	11.7	10.3	11.8	5.9	11.8	13.9	10.0	5.9	14.4	14.7	12.2
Viscosity Index	D 2270	165	144	99	179	160	146	166	142	155	118	155
Total Acid No., mg KOH/g	D 664	2.5	2.3	2.0	0.2	2.4	3.3	3.0	2.3	2.5	3.1	0.16
Total Base No., mg KOH/g	D 664	9.7	5.9	9.4	7.6	8.0	6.8	6.3	5.0	3.6	7.4	0.12
Flash Point, °C	D 92	208	218	246	244	215	209	224	232	198	230	221
Sulfated Ash, wt%	D 874	1.37	0.95	1.41	1.45	1.41	0.99	1.05	1.07	0.93	1.07	1.08
Elements, wt%												
Ba	XRF	Nil	Nil	Nil	0.84	Nil	Nil	Nil	0.24	Nil	Nil	Nil
Ca	XRF	0.37	Nil	0.35	Nil	0.37	0.26	0.24	0.03	0.17	0.20	0.28
Mg	AA	Nil	0.11	Nil	Nil	Nil	Nil	Nil	0.09	Nil	Nil	Nil
Zn	XRF	0.14	0.19	0.13	Nil	0.17	0.17	0.14	0.16	0.12	0.16	0.10
P	XRF	0.17	0.15	0.08	0.01	0.17	0.13	0.13	0.13	0.09	0.11	0.11
S	XRF	0.47	0.40	0.23	0.05	0.46	0.37	0.33	0.42	0.45	0.94	0.47
N	*	0.037	0.070	0.008	0.099	0.037	0.150	0.140	0.050	0.027	0.070	0.032

AA = Atomic Absorption Method
XRF = X-Ray Fluorescence Method
* = Chemiluminescent Method

15

2.3-liter multicylinder engine do not correlate in their wear response to lubricant formulations when using neat methanol fuel (Figure 4). In the single-cylinder engine, Lubricants B, C, D, and E had less iron wear than Lubricant A, while Lubricant G had approximately the same iron wear as Lubricant A. However, in the 2.3-liter multicylinder engine, all the lubricants had significantly more iron wear than did Lubricant A.

2. Lubricants

AFLRL work indicated that certain lubricant formulations appear to perform better than others but not at acceptable levels. Chui, and Millard and Chaibongsai had also reported extensive lubricant development work for use with methanol fuel.(13-15) Therefore, discussions were held with several lubricant manufacturers regarding the development of specialized lubricants to counteract the engine wear problems experienced with methanol fuel. As a result of these discussions, one lubricant manufacturer expressed a desire to provide experimental lubricant formulations for evaluation with alcohol-containing fuels. Throughout this phase, the manufacturer supplied a total of eleven lubricants for evaluation which were based on Lubricant A, the baseline lubricant in the previous AFLRL work. Lubricant A contained the following additives: calcium sulfonate detergent-dispersant, ashless phosphorus dispersant, alkyl zinc dithiophosphate, a dispersant-type viscosity index improver (polymethacrylate), and an ashless inhibitor. The compositional variations evaluated are shown in Table 4. The variations included changes in ashless dispersant, detergent-dispersant, viscosity index improver, antiwear agent, and ashless inhibitor chemistry. The physical properties of these lubricants are presented in Table 5.

a. Ashless Dispersant Effects

The summarized results of varying the ashless dispersant chemistry of Lubricant A are shown in Table 6. Lubricant A-1-2 was Lubricant A with the phosphorus dispersant replaced by a nitrogen (Type 1) dispersant. It resulted in less engine wear (599 ppm Fe) in the bore, ring, and cam areas. It appears that the ashless dispersant plays an important role in the lubricant formula-

16
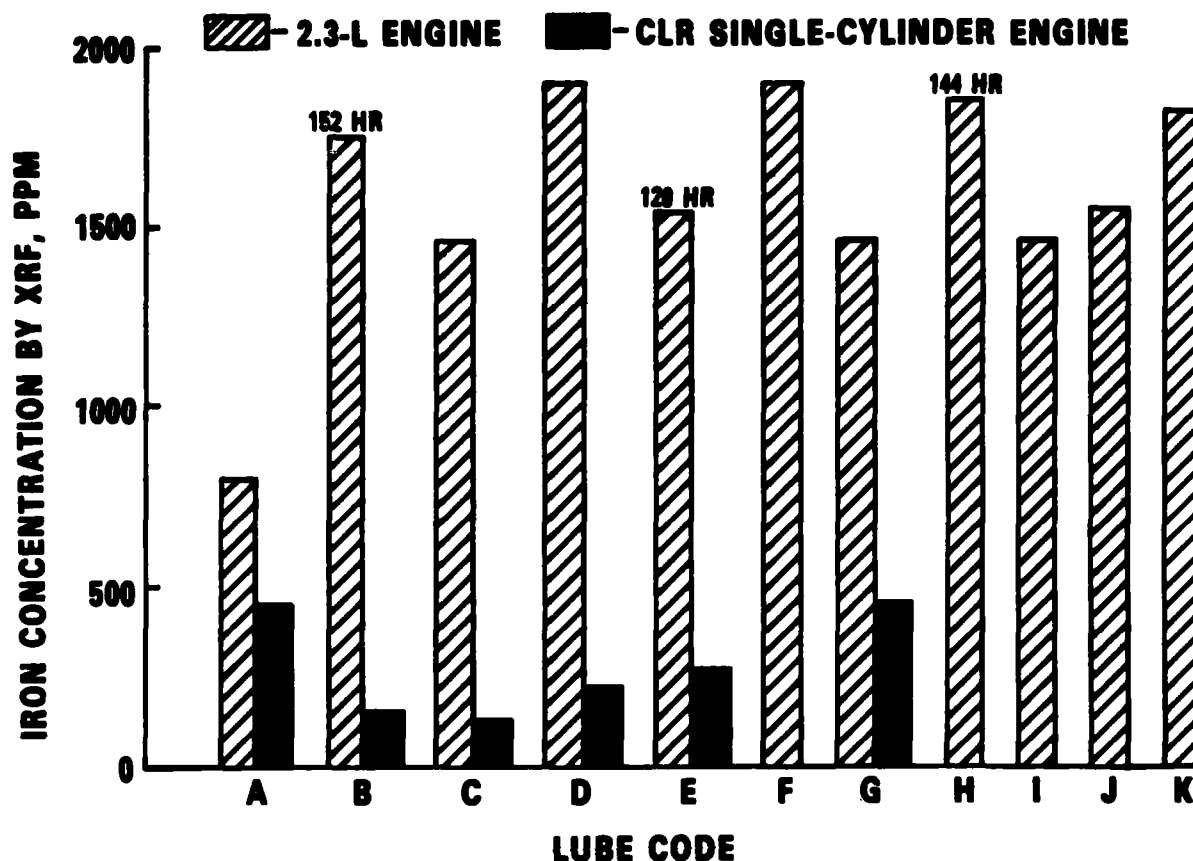
FIGURE 4. IRON WEAR METALS CONCENTRATION

TABLE 4. EXPERIMENTAL LUBRICANT VARIATIONS

Lubricant Number	Composition
A	P Disp, Ca Sulf, Alkyl ZDDP, Disp VII PMA & Ashless Inh (1)
A-1	A with N Disp-1
A-2	A with N Disp-1 & Mg Sulf (no Ca Sulf)
A-3	A with N Disp-1 & Aryl ZDDP
A-4	A with N Disp-1 & Shear Stable OCP VII
A-5	A with N Disp-1, Ashless Inh (2), & Friction Modifier
A-6	A with Mg Sulf (No Ca Sulf)
A-7	A with Increased Ca Sulf
A-8	A with no nitrogen or phosphorus disp (contained disp VII-PMA)
A-9	A with N Disp-2
A-10	A without VII, SAE-30
A-11	A with less shear stable OCP VII

TABLE 5. NEW LUBRICANT PROPERTIES

Oil Code	ASTM Test Method	A	Batch 1 A-1-1	Batch 2 A-1-2	Batch 3 A-1-3	A-2	A-3	A-4	A-5
K. Vis., 40°C, cSt	D 445	68.9	63.4	65.8	58.2	66.1	77.8	68.9	66.7
K. Vis., 100°C, cSt	D 445	11.7	11.2	11.3	10.4	11.5	11.9	10.6	10.8
Viscosity Index	D 2270	165	166	165	170	170	148	141	167
Total Acid No., mg KOH/g	D 664	2.47	2.03	2.28	2.55	2.58	1.98	2.08	2.03
Total Base No., mg KOH/g	D 664	9.73	8.93	9.75	9.89	7.25	9.53	9.11	9.71
Flash Point, °C	D 92	208	214	207	205	203	208	208	208
Sulfated Ash, wt%	D 874	1.37	1.40	1.43	1.44	1.04	1.42	1.40	1.42
Elements, wt%									
Ba, XRF		Nil	Nil	Nil	Nil	Nil	Nil	Nil	Nil
Ca, XRF		0.37	0.37	0.37	0.38	Nil	0.37	0.40	0.37
Mg, AA		Nil	Nil	Nil	Nil	0.22	Nil	Nil	Nil
Zn, XRF		0.14	0.13	0.13	0.13	0.11	0.13	0.13	0.13
P, XRF		0.17	0.11	0.11	0.10	0.14	0.09	0.10	0.10
S, XRF		0.47	0.47	0.48	0.46	0.43	0.44	0.47	0.46
N, *		0.037	0.088	0.088	0.090	0.069	0.094	0.072	0.094

Oil Code	Test Method	A-6	A-7	A-8	Batch 1 A-9-1	Batch 2 A-9-2	A-10	A-11
K. Vis., 40°C, cSt	D 445	64.7	63.8	53.6	62.9	67.3	88.3	72.1
K. Vis., 100°C, cSt	D 445	11.1	11.1	9.8	10.9	11.5	10.3	11.1
Viscosity Index	D 2270	166	167	170	167	166	97	146
Total Acid No., mg KOH/g	D 664	2.52	2.47	2.39	2.61	1.95	2.30	2.26
Total Base No., mg KOH/g	D 664	7.54	14.57	7.48	8.22	7.20	9.31	8.97
Flash Point, °C	D 92	206	210	209	199	217	234	214
Sulfated Ash, wt%	D 874	1.07	1.90	1.40	1.41	1.39	1.35	1.34
Elements, wt%								
Ba, XRF		Nil	Nil	Nil	Nil	Nil	Nil	Nil
Ca, XRF		Nil	0.54	0.38	0.38	0.37	0.36	0.37
Mg, AA		0.18	Nil	Nil	Nil	Nil	Nil	Nil
Zn, XRF		0.11	0.12	0.13	0.13	0.12	0.12	0.11
P, XRF		0.15	0.15	0.11	0.11	0.08	0.14	0.14
S, XRF		0.52	0.50	0.38	0.42	0.47	0.67	0.51
N, *		0.030	0.031	0.034	0.090	0.064	0.025	0.022

AA = Atomic Absorption Method
XRF= X-Ray Fluorescence Method
* = Chemiluminescent Method

18

TABLE 6. ASHLESS DISPERSANT EFFECTS WITH METHANOL FUEL

			Modified V-D Test Results							
			Avg Ring Gap Incr, mm		CAM			Deposits 10=Clean		
Lube Code	Lubricant Composition	Avg Top Bore Incr, mm	No. 1	No. 2	Follower Wt Loss Avg, g	Lobe Wear, mm	Used Oil Fe, ppm	Avg Sludge	Avg Varn	Avg P.Varn
A	P disp., Ca Sulf, alkyl ZDDP, Disp. VII-PMA, Ashless Inhib. -1	0.0660	0.178	0.102	0.06	0.06	806	9.74	9.59	9.90
A-1-2	A with Nitrogen Disp. -1 BATCH-2	0.0350	0.102	0.05	0.03	0.03	599	9.65	9.28	9.95
A-1-3	A with Nitrogen disp. -1 BATCH-3	0.0610	0.279	0.152	0.01	0.02	1413	9.73	9.43	9.84
A-9-1	A with Nitrogen disp. -2 BATCH-1	0.0356	0.152	0.114	0.03	0.04	442	9.70	9.90	9.57
A-9-2	A with Nitrogen disp. -2 BATCH-2	0.0457	0.178	0.102	0.23	0.10	1500	9.72	9.25	9.50
A-8	A with no Ashless disp. (VII-PMA disp. type)	0.0889	0.279	0.152	0.08	0.11	1456	9.51	8.55	9.22

tion in combating methanol-related wear. Additional experimentation is needed to define the optimum ashless dispersant chemistry for use with methanol fuel and to explain differences in performance of various batches of the same lubricant formulation.

b. Detergent Dispersant Effects

The summarized results of varying the detergent/dispersant chemistry of Lubricant A are shown in Table 7. The effect of increasing the calcium sulfonate content of Lubricant A was investigated. Overall, it appears that the overbased detergent-dispersant additive plays an important role in controlling methanol-related engine wear. Calcium sulfonate was found to be more effective than magnesium sulfonate. Also, it was found that increasing

19

TABLE 7. DETERGENT/DISPERSANT EFFECTS WITH METHANOL FUEL

Lube Code	Lubricant Composition	Modified V-D Test Results								
		Avg Top Bore Incr, mm	Avg Ring Gap Incr, mm		CAM		Used Oil Fe, ppm	Deposits 10=Clean		
			No. 1	No. 2	Follower Wt Loss Avg, g	Lobe Wear, mm		Avg Sludge	Avg Varn	Avg P.Varn
A	Ca Sulf, P Disp. alkyl ZDDP, Disp VII-PMA, Ashless Inhib. -1	0.0660	0.178	0.102	0.06	0.06	806	9.74	9.59	9.90
A-7	A with increased Ca sulf	0.0533	0.254	0.076	0.10	0.03	881	9.71	9.11	9.67
A-6	A with Mg sulf (no Ca sulf)	0.1118	0.432	0.127	0.02	0.46	1440	9.72	9.77	9.86
A-2	A with Mg sulf + Nitrogen disp. -1 (120-Hr. test)	0.1194	0.305	0.152	0.02	0.05	1734	9.22	8.90	9.85

the calcium sulfonate content by approximately 50 percent was not effective in reducing engine wear. The lack of effectiveness of increasing detergent-dispersant content again demonstrates that the wear does not result from a depletion of the additives.

c. Viscosity Index Improver Effects

The summarized results of varying the viscosity index improver chemistry of Lubricant A are shown in Table 8. Overall, these tests appear to indicate that VII variations had some effect on bore wear and an even greater effect on cam area wear when using methanol fuel.

d. Miscellaneous Additive Effects

The summarized results of varying the zinc additive chemistry and varying the inhibitor additive are shown in Table 9. It is generally accepted that the Sequence V-D 2.3-liter engine is sensitive in the valve train area to the

TABLE 8.   VI IMPROVER EFFECTS WITH METHANOL FUEL

Lube Code	Lubricant Composition	Modified V-D Test Results								
		Avg Top Bore Incr, mm	Avg Ring Gap Incr, mm		CAM		Used Oil Fe, ppm	Deposits 10=Clean		
			No. 1	No. 2	Follower Wt Loss Avg, g	Lobe Wear, mm		Avg Sludge	Avg Varn	Avg P.Varn
A	Disp VII-MPA, Ca sulf, P disp. alkyl ZDDP, ZDDP, Ashless Inhib. -1	0.0660	0.178	0.102	0.06	0.06	806	9.74	9.59	9.90
A-11	A with OCP VII (less shear Stable)	0.0457	0.203	0.127	0.15	0.13	1258	9.69	9.46	9.84
A-4	A with OCP VII (shear stable) + Nitrogen disp. -1	0.0533	0.254	0.102	0.01	0.02	585	9.73	9.88	9.44
A-10	A with no VII (SAE 30)	0.0432	0.152	0.102	0.16	0.09	1157	9.57	9.13	9.72

TABLE 9.   MISCELLANEOUS ADDITIVE EFFECTS WITH METHANOL FUEL

Lube Code	Lubricant Composition	Modified V-D Test Results								
		Avg Top Bore Incr, mm	Avg Ring Gap Incr, mm		CAM		Used Oil Fe, ppm	Deposits 10=Clean		
			No. 1	No. 2	Follower Wt Loss Avg, g	Lobe Wear, mm		Avg Sludge	Avg Varn	Avg P.Varn
A	Ashless Inhib. -1 alkyl ZDDP, Ca sulf, P-disp. Disp VII-PMA	0.0660	0.178	0.102	0.06	0.06	806	9.74	9.59	9.90
A-5	A with Ashless Inhib. -2 + Friction Modifier, Nitrogen disp. -1 (140-Hr)	0.1194	0.356	0.203	0.24	0.11	2242	9.70	8.50	9.74
A-3	A with Aryl ZDDP + Nitrogen disp. -1	0.0356	0.254	0.178	0.19	0.09	1580	9.66	9.05	9.98
A-1-2	A (alkyl ZDDP) with Nitrogen disp. -1 BATCH-2	0.0350	0.102	0.05	0.03	0.03	599	9.65	9.28	9.95
A-1-3	A (alkyl ZDDP) with Nitrogen disp. -1 BATCH -3	0.0610	0.279	0.152	0.01	0.02	1413	9.73	9.43	9.48

type of zinc antiwear additive when using unleaded gasoline fuel.(16) It appears that valve train area wear resulting from aryl zinc may occur with both methanol fuel and unleaded gasoline. Use of methanol fuel does not have any apparent effect on the effectiveness of the zinc-containing additives in controlling cam and valve train wear.

Based on this work, it appeared that the increased wear experienced with methanol could be reduced through proper lubricant formulation. However, the best lubricant tested resulted in wear levels twice that of unleaded gasoline. This wear level is not considered acceptable for unrestricted use. Without a more fundamental understanding of which mechanisms were responsible for the increased wear, the development of effective lubricant and additive formulations would be potentially expensive and time consuming.

B. Mechanism Studies

A series of experiments were conducted to identify the mechanisms and chemical species responsible for the increased wear observed with methanol.

The first experiment aimed at identification of the wear mechanism consisted of operating two identical CLR engines using a common oil sump and lubricant system.(17) One engine was operated on methanol while the other was run on unleaded gasoline. Both engines were run simultaneously with identical operating conditions. The reasoning was that if lubricant degradation or contamination was the cause of the wear, both engines would show elevated wear rates. At the completion of the test, both engines were dismantled and measured for wear. The cylinder bore and piston ring wear in the methanol engine was twice that of the gasoline engine, thus suggesting that lube oil degradation or contamination is not the controlling factor in the wear mechanism. Instead, it seemed more probable that large quantities of methanol entered the cylinder as a liquid and wetted the cylinder walls, suggesting the possibility of a removal of the lubricant film and/or a direct chemical attack of the metal surfaces.

22

To investigate the role of liquid methanol, the CLR engine was fitted with a methanol vaporization system.(17) The methanol vaporization system consisted of a boiler and a superheater section, both of which were heated electrically. When operated on the vaporization system, methanol vapor was supplied at the intake valve of the engine at a state which had a sufficient degree of superheat to ensure that no condensation could occur in the combustion chamber (Table 10). Operating in this mode eliminated the possibility of having liquid methanol present in the combustion chamber. The wear rates for both the unleaded gasoline test and the vaporized methanol test were both very low, as indicated by the accumulation of iron in lube oil samples taken every 4 hours during the tests. The baseline methanol test using a carburetor showed an overall higher wear rate, especially during the final 12 hours of the test. During the baseline test, however, the water and methanol concentrations in the lube oil became excessive, with, at one point, the lube at one point, the lube oil accounting for only 39 percent of sump contents.(17) It was thought that the high level of dilution may have contributed to the high wear rates, at least during the final hours of the test. This clouded the results of this series of engine tests.

TABLE 10.   OPERATING CONDITIONS FOR CLR METHANOL VAPORIZATION TESTS

RPM	1550±25
Load	1.86±0.15 kW (2.5±0.2 Hp)
Air/Fuel Ratio	5.0±0.2
Oil Temperature	57°C (135°F)
Coolant Temperature	46°C (115°F)
Superheater Outlet Temperature	149°C (300°F)
Superheater Outlet Pressure	86 kPa (12.5 psi)

In another series of tests, the CLR engine was equipped with a blowby gas sampling system. The design and use of this system were reported previ-

ously.(11,16,18) The results of the other CLR engine tests indicated that
the wear mechanism was not due to lube oil degradation or dilution. The pur-
pose of this test was to determine qualitatively the composition of the meth-
anol combustion products present in the ring zone.

Analysis of samples collected from the methanol-fueled engine showed concen-
trations of methanol, methane, formaldehyde, formic acid, acetaldehyde, and
acetic acid. It appeared that formaldehyde, formic acid, and probably meth-
ane were products of incomplete combustion of methanol. Of most concern was
the formic acid, because of its potential to cause corrosion. If the formic
acid is formed at the cylinder wall, or somehow migrates to the cylinder
wall, it could react with the cast-iron liner.

Using the 2.3-liter Sequence V-D engine, a series of 20-hour steady-state
tests (Table 11) were performed to observe whether increased intake air
temperatures with methanol or increased prevaporization of methanol could
reduce engine iron wear accumulation. These tests were conducted to confirm
the results obtained with the CLR engine and to examine the impact of intake
mixture heating. The first test was conducted with exhaust gas heating the
intake manifold rather than using engine coolant as the heat source. This
increased the average air/fuel intake manifold temperature from 10.2°C
(50.4°F) to 19.9°C (68.8°F), so apparently no significant increase in vapor-
ization was achieved. Also, no decrease in iron wear occurred, as the data
were within the range of previous 20-hour tests (Figure 5).

A fuel vaporizer was then built using the exhaust gas heat to vaporize the
methanol. The engine was started with unleaded gasoline. When the exhaust-
heated vaporizer was operating at sufficiently high temperature, the unleaded
gasoline was turned off, and the engine switched to vaporized methanol. This
arrangement appeared to operate successfully because of the increased intake
air/fuel temperature without the heated intake air (Table 11). The results
of prevaporizing methanol shown in Figure 5 appeared to slightly decrease the
iron wear level. It was felt that possibly incomplete vaporization or con-
densation of methanol during the compression stroke could have occurred.

24

TABLE 11. AIR/FUEL INTAKE TEMPERATURE WITH METHANOL
USING VARIOUS MIXTURE HEATING SYSTEMS

Test Hardware Configuration	Inlet Air Temp., °C (°F)	A/F Mixture Temp. at Engine Oil-in Temperatures, °C (°F)	
		46.1°C (115°F)	98.9°C (210°F)
Coolant-heated intake manifold	29.4 (85)	10.2 (50.4)	15.6 (60.1)
Exhaust-heated intake manifold	29.4 (85)	19.9 (67.8)	20.8 69.4)
Heated-intake air	93.3 (200)	44.4 (112)	ND
Exhaust-heated fuel vaporizer	29.4 (85)	47.8 118)	50.2 (122.4)
Exhaust-heated fuel vaporizer plus heated intake air	93.3 (200)	72.8 (163)	ND

ND = Not Determined

LUBRICANT A

○ COOLANT HEATED INTAKE MANIFOLD
● EXHAUST HEATED INTAKE MANIFOLD
△ SONIC CARBURETOR
□ VAPORIZED METHANOL
■ VAPORIZED METHANOL + HEATED INTAKE AIR
PLUS 200°F INTAKE AIR
— —AVERAGE OF ALL TESTS (BASELINE)
——PHILLIPS J UNLEADED GASOLINE

AREA BOUNDED BY EIGHT
PREVIOUS BASELINE TESTS

ENGINE OIL IN TEMPERATURE
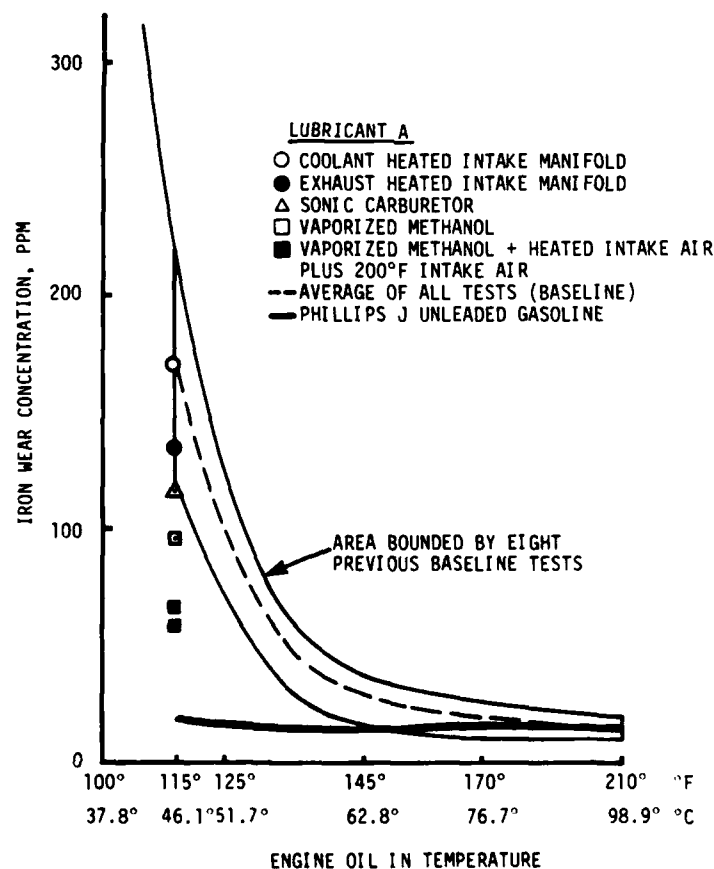
FIGURE 5. EFFECTS OF INDUCTION SYSTEM MODIFICATIONS
ON ENGINE IRON WEAR

25

have occurred. Consequently, the 20-hour steady-state test was conducted using the heated carburetor intake air and the exhaust-heated methanol vaporizer. This combination appeared to operate successfully because the intake air/fuel temperature increased to 72.8°C (163°F), well above the dew point for a stoichiometric methanol/air mixture. Figure 5 shows that the iron wear was somewhat lower and was outside the envelope of the previously bounded tests. It was concluded that the achievement of complete vaporization of methanol reduced the iron wear, but not to unleaded gasoline level.

C. Discussion of Engine Experiments

Based upon the results of the various engine experiments, it appears that the wear mechanism is related to the presence of liquid methanol on the cylinder walls. This is suggested by the results of the methanol/vaporization tests in which the wear rates were substantially reduced when the liquid methanol was eliminated from the combustion chamber.

It would be expected that lube oil dilution by methanol or methanol combustion products would also be reduced by using vaporized methanol. This is indeed the case, but the tests with the single oil system shared by two engines indicated that lube oil dilution and/or degradation are not the controlling factors in the wear mechanism.

D. Spinning Disc Combustor Tests

A spinning disc combustor was constructed to examine the corrosive mechanism of wear. The device, shown schematically in Figure 6, consisted of a spinning disc atomizer mounted inside a water-cooled cast-iron cylinder liner.

Methanol was introduced at the center of the spinning disc with atomization occurring as a result of centrifugal force. Ignition was accomplished using a methane pilot flame located at the disc discharge. The flow of combustion air was controlled by adjusting the height of the liner above the condensate reservoir.

26
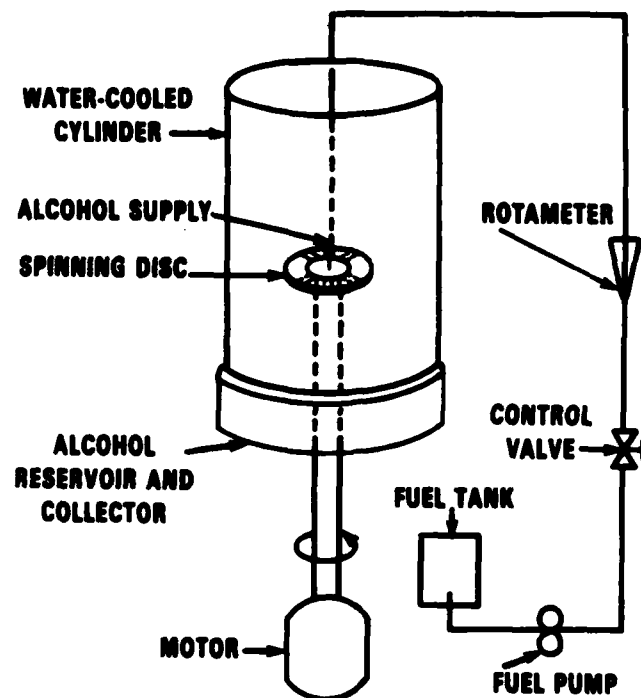
FIGURE 6. SPINNING DISC COMBUSTION SCHEMATIC

The inside surface temperature of the cylinder liner could be changed by controlling the flow of cooling water through a water jacket surrounding the liner. In addition to containing the flame, the cooled cylinder liner: (1) quenched the burning fuel droplets as they impacted the cold wall; (2) caused condensation of some of the combustion products of the methanol; (3) provided a surface upon which a liquid boundary was formed; and (4) provided a chemically active surface upon which and with which the combustion products could react. The liquid products collected on the wall were allowed to drip into the condensate reservoir located beneath the cylinder. Samples thus collected were removed and analyzed for chemical composition.

Preliminary tests showed that the liquid condensate caused severe corrosion of the cast-iron cylinder. It was observed that at surface temperatures above 70°C the collection of condensate ceased.

A series of experiments directed at identifying corrosive materials in the condensate sample, was performed using the cast-iron cylinder liner with a freshly honed inside surface. The liner surface temperature, in the region of the disc discharge, was maintained below 51°C.

The condensate from the spinning disc apparatus was analyzed for water, methanol, formaldehyde, formic acid, total acidity, and iron. Iron was found in the condensate sample in the form of a rusty red-colored precipitate which could be separated from the liquid by light centrifuging. A portion of the iron-containing precipitate was mixed with potassium bromide powder; this was compressed into a pellet and used as an optical absorption cell for analysis by infrared spectroscopy.

The condensate consisted mainly of water and methanol. The amount of water in the condensate samples ranged from about 15 to 65 percent by volume depending on the cylinder wall temperature in the spinning disc apparatus. The samples were acidic (total acid number of about 1) and contained relatively small amounts of formaldehyde and rust-colored precipitate. X-ray fluorescence revealed that the rust-colored precipitate contained about 33 percent iron, which was considerably less iron than would have been expected if the precipitate was either ferric hydroxide, $Fe(OH)_3$ (52.3 percent iron) or iron oxide, Fe_2O_3 (70.6 percent iron). The infrared spectrum of the precipitate is shown in Figure 7A. The strong absorption bands at 6.4 and 7.3 micrometers are characteristic of the formate ion. To confirm this analysis, the second infrared spectrum shown in Figure 7B was taken of a sample of iron formate $[(Fe(HCOO)_3]$ that was prepared in the laboratory. The iron content of pure iron formate is 29.3 percent. The value of 33 percent found by X-ray fluorescence suggests that the rust-colored precipitate is a mixture of pure iron formate and ferrichydroxy-diformate, $Fe(OH)(HCOO)_2$, which contains 34.3 percent iron. These results show that corrosion of the cylinder wall is due to reactions with formic ion formed as a result of combustion of methanol.

It is apparent from the experimental results that the corrosive wear in engines operating at low temperatures on methanol is due to attack by formic acid. The formic acid appears to react rapidly with the cast-iron cylinder

WAVELENGTH IN MICROMETERS
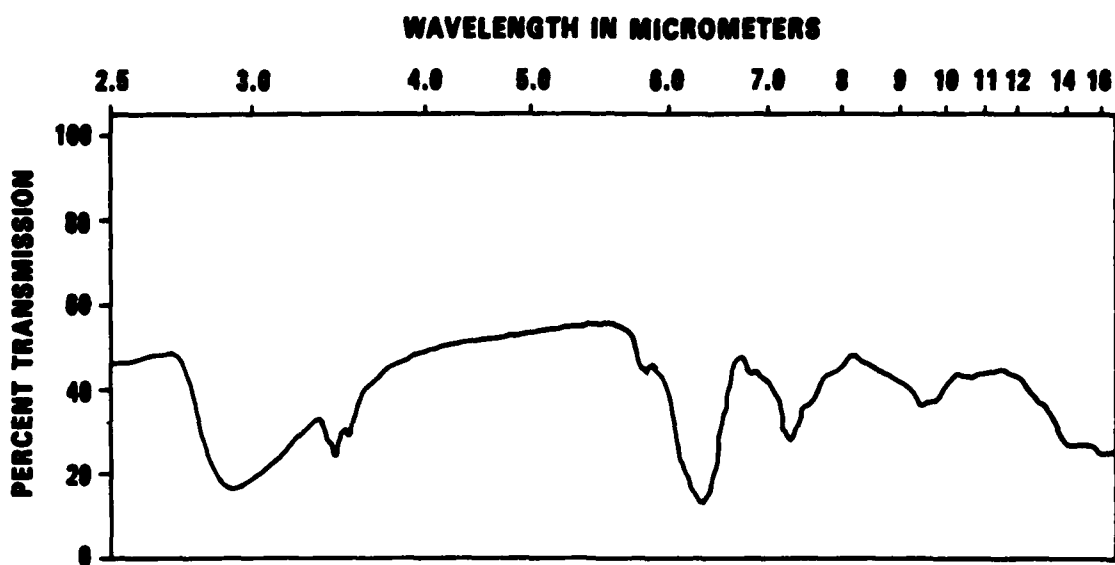
(A) PRECIPITATE IN CONDENSATE FROM SPINNING DISC EXPERIMENT

WAVELENGTH IN MICROMETERS
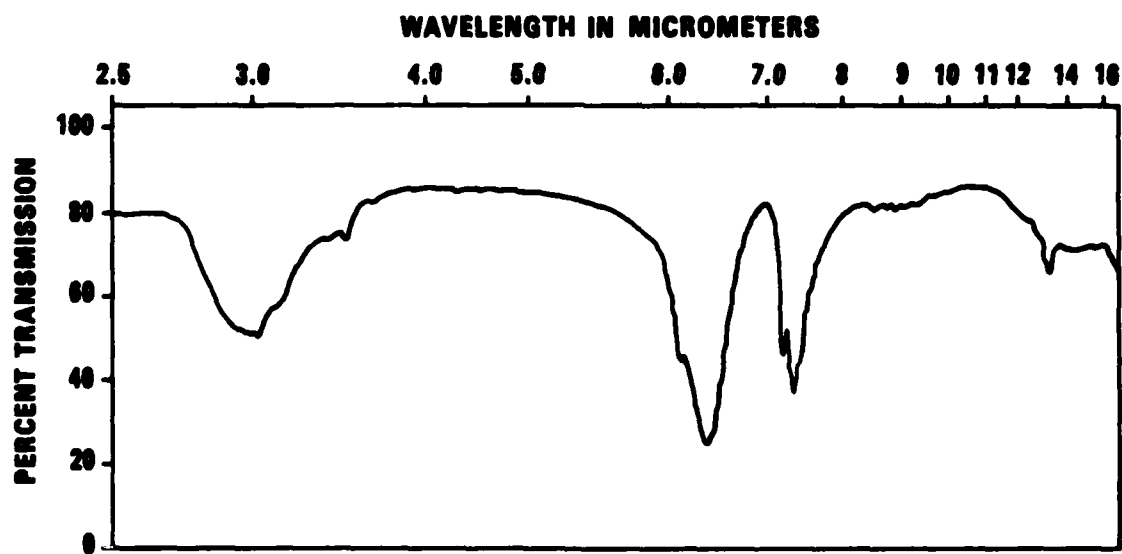
(B) IRON FORMATE PREPARED IN LABORATORY

FIGURE 7.   INFRARED SPECTRA SHOWING PRESENCE OF FORMATE ION

29

wall to form iron formate which eventually is removed from the surface by the piston ring. It seems that most of the formic acid reacts with the cylinder wall because only trace amounts of acid are found in the lubricant and blowby.

The mechanism for the formation of formic acid was as yet uncertain.* The experiments in the spinning disc apparatus suggest that the surface of the cylinder wall may play a role in the formation and/or decomposition of formic acid. If formic acid forms in the gas phase, the surface could act as a decomposition catalyst.

The mechanism for the formation of formic acid does not appear to be surface related, but this cannot be ruled out. The cylinder wall is relatively cool as the flame approaches so that the surface-catalyzed oxidation of stable combustion intermediates such as formaldehyde would seem to be a slow process that is unlikely to be significant in the duration of the combustion stroke. Instead, it appears that the precursors to formic acid are formed in the quench layer as the flame, rich in free radicals, approaches.

To evaluate a theory put forward by Ernst, et al. (19), a nitrogen-free engine test was performed to determine the importance of nitric acid in the corrosion of the upper cylinder bore and ring areas of methanol-fueled engines. Recognizing the difficulties of detecting nitrogen dioxide or nitric acid in the combustion chamber, a less ambiguous approach for determining the importance of nitric acid was to conduct a nitrogen-free engine experiment. The 2.3-liter engine and 20-hour test cycle were selected for the experiment because of the available baseline data and the consumption of the minimum amount of nitrogen-free gas. A 23 percent argon/56 percent carbon dioxide/21 percent oxygen mixture was used because it provided a working fluid that was both thermodynamically and chemically similar to air. This mixture provided the same specific heat ratio, gamma = 1.38, as air at room temperature. However, it is important to note that the gamma of that mixture decreases relative to air at higher temperatures because the specific

---

* One possible mechanism for the formation of formic acid from methanol oxidation is discussed in the appendix.

heat of carbon dioxide is more dependent on temperature than that of nitrogen. This reduces the adiabatic compression temperature, the adiabatic flame temperature, and the thermodynamic efficiency of the cycle. The test results gave all indications that the engine performance and combustion efficiency were similar to those observed in baseline tests with air. Analysis of exhaust emissions, exhaust condensate, and blowby condensate showed that only trace amounts of nitrogen oxides were present in the engine. Wear measured in terms of iron buildup in the lubricant was found to be essentially the same in the nitrogen-free test as that detected in baseline engine tests combusting methanol-air mixtures. Thus, both theory and experimental results rule out the importance of nitric acid in the corrosion of the upper cylinder bore and ring areas of methanol-fueled engines.

In looking for clues to the wear mechanism, the temperature dependence of the wear metals accumulation in the lubricant was studied. In the engine tests, the rate of wear metals accumulation in the lubricant was strongly dependent on the temperature and could be expressed as

$$\ln (\text{iron conc.}) = b/T + C \qquad (1)$$

where T is the oil temperature entering the gallery in degrees Kelvin, b is the temperature coefficient, and C is a constant. It is important to note that coolant temperature was closely matched to the oil temperature in the engine tests used to reach the above conclusion. The mathematical form of Equation 1 is used to describe properties such as vapor pressure (Clausius Chaperon Equation), chemical equilibrium, and reaction rates. The magnitude of the temperature coefficient, b, is usually indicative of the property which is important in the process. Using wear metals accumulation from several engine tests, the value of b was found to be 10,400. This was first thought to be the activation energy, E/R, of a chemical reaction (3), but, based on other evidence, it seemed more probable that the temperature dependence was related to the evaporation of fuel from the cylinder wall. When the engine tests using methanol containing 11 percent water were performed, the rate of wear metal buildup in the lubricant increased about five

31

fold. On the other hand, prevaporization of the anhydrous methanol inducted by the engine reduced the rate of wear metal accumulation by about 50 percent of that measured in neat liquid methanol-fueled engine tests.(1) If evaporation of liquid from the cylinder decreased wear, it seemed that the use of prevaporized methanol would reduce the wear to the baseline observed with unleaded gasoline. Upon examination of the prevaporization tests, it was concluded that it was possible that some of the methanol vapor could have condensed on the relatively cool cylinder wall. Based on calculations (20) of the dew point of the compressed methanol vapor/air mixture and the approximate temperature of the cylinder wall, it was concluded that some methanol vapor could have condensed on the cylinder wall.

In light of the above observations, a simple model (20), based on the Stefan Equation (21), for the rate of evaporation of liquid methanol from a surface was used to predict the temperature dependence of the wear metal accumulation rate. In comparing the model and the test results, the wear rate was simply assumed to be inversely proportional to the rate of evaporation of methanol from the cylinder wall. A correlation of the calculated wear rates with temperature using Equation 1 gave a temperature coefficient, b, of 10,490, which was essentially the same as that found in the correlation of the experimental values. This suggests strongly that liquid on the cylinder wall is a criteria in the wear mechanism.

Realizing the significance of a liquid methanol layer on the cylinder wall, it seemed reasonable to assume that corrosion could be caused by deleterious combustion intermediates which diffuse to the wall and dissolve in the liquid film. Experiments carried out in a spinning disc apparatus support this theory. In an earlier engine test using a blowby diversion piston, it was found that the blowby condensate also contained formaldehyde and formic acid. These results strongly suggested that formic acid played a major role in the corrosion mechanism. Recently, Otto, et al. (22), have reached the same conclusion by exposing a steel coupon to methanol combustion products in a pulse flame combustor. They also conclude that rust formation is triggered by formic acid in the exhaust, first forming ferrous formate which then reacts with liquid water and oxygen from the gas phase to produce FeOOH and

32

Fe_3O_4. Rust formation decreased sharply when the temperature of the steel coupon was raised above the dew point at which moisture condenses from the exhaust gas.

Other corrosion processes have been proposed to explain the wear found in methanol-fueled engines. Fuel impurities such as chlorine are known to cause corrosion in methanol-fueled engines.([6]) Apparently, the chlorine is converted in the combustion process to hydrogen chloride, which combines with water vapor and condenses on the cylinder wall. Similarly, sulfur contamination might cause sulfuric acid to form. These corrosion processes are easily eliminated by excluding chlorine and sulfur from the fuel through appropriate storage and maintenance procedures.

A search is made for deleterious species formed by the combustion of low molecular weight alcohols. This includes an examination of the combustion intermediates found in partially burned shallow pools and burning fuel droplets. The kinetics of the corrosion process is examined, and a possible mechanism for the formation of formic acid in the combustion of alcohols is proposed.

The engine cylinder walls are usually covered by a thin layer of oil. This lubricant film provides separation between the sliding piston rings and the cylinder wall during engine operation, while the additives carried by the oil produce organometallic films on the metal surfaces to provide wear protection during those periods of boundary lubrication. Also, the lubricant contains additives which are intended to react with reactive combustion products and thus protect the engine from corrosive wear. The greatly increased wear that occurred with methanol fuel indicated that these lubricant formulations were inadequate to prevent corrosive attack by the methanol combustion products. Variations in lubricant additive chemistry were shown to provide some increase in protection; however, the high wear rates still observed raised questions as to how the methanol liquid or its combustion intermediates were able to penetrate the physical barrier of the lubricant film.

During normal engine operations with gasoline fuels, any fuel droplets that reach the cylinder walls are dissolved in the oil film. This may reduce the viscosity of the liquid on the wall but would have little effect otherwise. Any ruptures of the lubricant film would heal through flow of oil, even if gasoline were present. However, methanol and the hydrocarbons typically used as lubricants are essentially immiscible. There was concern that methanol liquid which reached the cylinder walls through ruptures in the oil film would adsorb onto the wall, reducing the ability of the lubricant to wet that area. This would result in reduced adhesive wear protection in that area, plus would form a pathway for corrosive materials to penetrate the barriers normally present.

III. OBJECTIVE

Based on previous studies discussed in the Introduction, it was apparent that either liquid methanol or some combustion condensate on the cylinder wall was responsible for the corrosive wear in methanol-fueled engines. It seemed that corrosive products were formed as the result of incomplete combustion near the relatively cool cylinder wall. The corrosive combustion products diffused to the cylinder wall and dissolved in the liquid layer. It was also hypothesized that the highly polar liquid methanol would displace the protective lubricant film and expose the metal to the corrosive combustion products.

Several related experiments were performed during the course of this project to determine the various physiochemical aspects of the wear mechanism. The objectives of this work were to: (1) determine if methanol significantly interferes with the formation of oil films, i.e., alters the normal lubricant/metal surface interaction,: (2) identify the combustion products formed from alcohols that cause corrosion of cast iron,: (3) determine the properties of alcohol combustion residues and elucidate the mechanism of transport of combustion products to the cylinder wall,: (4) determine the significance of each combustion product in the corrosion mechanism, and: (5) investigate the kinetics of formation of deleterious combustion products such as formic acid and peroxides.

IV. EXPERIMENTAL PROCEDURES

Although the various phases of experimental work performed during the course of this project were related to the mechanism of wear in methanol-fueled engines, the actual experimental methods and analytical techniques varied considerably. Rather than attempt to categorize and describe them in this section of the report, the procedures used in each experiment are discussed as part of the Results and Discussion section.

V. RESULTS AND DISCUSSION

A. Methanol Surface Reaction Measurements

In one approach, engine wear was simulated and surface reaction products formed by employing an LFW-1 wear test machine to produce wear conditions similar to the top of piston travel region of an actual engine. Specimens were tested under two conditions. The baseline tests were performed using conventional lubrication. Although similar to the baseline series, the second series of tests had methanol applied to the wear surface. Conditions were varied to allow testing both within the boundary lubrication mode and within hydrodynamic mode. Test specimens were analyzed using X-ray diffraction, energy-dispersive X-ray spectroscopy (EDS), and electron spectroscopy for chemical analysis (ESCA). Both X-ray diffraction and EDS analysis failed to detect any differences between the specimens prepared with oil and the specimens prepared with oil-methanol. This was probably due to the surface reaction product's layers being too thin to be detected by these techniques. ESCA examination of the specimens showed significant differences in oxygen content of the surface layers. The specimens produced with oil-methanol had 39.5 atomic percent oxygen content, while the samples prepared with oil had only 23.4 atomic percent oxygen content in the surface layer. The oxygen appeared to be bound to the surface layer in the form of oxide and carbonyl groups.

A second approach to formation of surface reaction products involved lapping of specimens using a slurry of fine abrasive and test fluid. The thin layer of metal that had reacted with the atmosphere was removed from the specimen by abrasion action, and the freshly exposed metal surface was immediately subjected to the reactive effects of the test fluid. After the lapping operation, samples were placed on a heated test block and a measured drop of oil was placed on the sample surface. Measurement of oil drop spread rate indicates the effects of surface reaction products on surface wettability by lubricating oil. No visual change was noted in the oil-lapped specimens, but the methanol-lapped specimens appeared to have a slight blue color after lapping which intensified for several hours during storage. Methanol-lapped specimens which exhibited the bluing effect had reduced oil drop spread rates as compared to the oil-lapped specimens, indicating reduced wettability by oil. This could be a factor in the increased wear observed in alcohol-fueled engines, since good oil film continuity is coincident with good wettability and is required for proper lubrication.

B.   Identification of Combustion Intermediates

The experimental approach used to examine the formation and solubility of combustion intermediates and products in alcohols was based on the work of Seshadri (23) on the structure and extinction of laminar diffusion flames above liquid fuels. Seshadri (23) established a flat flame above a liquid pool of methanol and measured concentration profiles of combustion products and stable intermediates between the liquid surface and slightly beyond the flame zone. All the species observed previously including CO_2, CO, H_2O CH_4, C_2H_2, C_2H_4, C_2H_6, and HCHO (24,25) were detected by his gas sampling probe and gas chromatograph system. However, of some surprise, methylformate, $HCOOCH_3$, was also among the species detected. The concentration of methyl-formate was highest near the surface of the liquid. This was contrary to the concentration profiles of the other species, which had higher concentrations near the flame zone. The concentration gradient indicated that the methyl-formate was actually evaporating from the liquid methanol. Seshadri (23) concluded that the methylformate must have been an impurity in the methanol used in the experiment. However, if formic acid had been detected, the

36

formation of methylformate would not seem too improbable. Since low concentrations (<1000 ppm) of formic acid are difficult to measure by gas chromatography, it is reasonable to assume that it was below the detection limit. In a March 1984 unpublished collaborative effort between Drs. Seshadri and Naegeli, a second attempt was made to detect formic acid in the gas phase above liquid methanol. While measurements using gas chromatography gave no indication of formic acid in the gas phase, ion chromatographic analysis of the liquid phase showed that formate ions were present.

In view of these results, two experimental approaches were used to investigate the liquid phase composition of alcohols during their combustion. These experiments consisted of (1) quenching burning droplets of methanol in water and analyzing the water-soluble products, and (2) burning alcohol pools in various containers and analyzing the combustion residues. The corrosive nature of the combustion products was examined in Experiment 1 by allowing burning methanol droplets to interact with cast iron and in Experiment 2 by burning alcohol in a cast iron container. Basically, the combustion products and corrosion products found in both experiments were the same. After preliminary results were obtained on both experiments, it became clear that the pool-burning approach (Experiment 2) was most conducive to study and it appeared to relate best to the problem of cylinder bore and ring corrosion.

Combustion residues were first found when shallow pools of methanol were burned to extinction in an evaporating dish which was cooled in a bath of tap water. In subsequent experiments, shallow pools of low molecular weight alcohols were burned to extinction in separate containers made of cast iron, stainless steel, and aluminum. The combustion residues caused significant corrosion of cast iron, but did not affect the stainless steel and aluminum containers.

Several analytical techniques were used to measure the composition of the residues formed from burned alcohol pools. Sample size was an important criteria in analysis such as pH because residue volumes were generally much less than 10 percent of the initial fuel volume. As a result, a dual electrode microprobe was used to measure the pH of the residue.

Used in the analysis was a Hewlett-Packard model 5700, a Grow Mac thermo-conductivity detector, and gas chromatograph equipped with temperature pro-gramming. A 1.8 meter by 6.4 millimeter glass chromosorb 107 column was used to analyze the residues for possible compounds including water, alcohol, formaldehyde, acetadehyde, methylformate, and formic acid. A Beckman model ACTA CIII spectrophotometer was used to measure formaldehyde and peroxides in the residues. Formaldehyde was determined by the spectrophotometric method described by Bricker and Johnson (26) using chromotropic acid reagent. Formaldehyde was indicated by a purple coloring which absorbed at 570 nm. Peroxides were determined by the spectrophotometric method described by Egerton, et al. (27) using titanous chloride reagent. Peroxides produced a yellow coloring that absorbed at 410 nm. The method was particularly suited for measuring hydrogen peroxide in aqueous solutions. Egerton, et al. pointed out that there could be some problem in analyzing peroxides when formal-dehyde was present because hydroxyperoxides are formed.

The method was tested on aqueous solutions of hydrogen peroxide and similar solutions containing formaldehyde. When the titanous chloride reagent was added to the aqueous hydrogen peroxide solution, the yellow color developed immediately; thereafter, the optical density remained constant.

In the solution containing formaldehyde, the yellow color developed slowly, and it took about 30 minutes before the optical density reached the same value obtained with the formaldehyde-free sample. The results showed that the peroxide contents of samples containing formaldehyde could be determined if about 30 minutes were allowed for color development.

Ion chromatography (28) was used to determine the concentrations of formate and acetate ions in the residues. The term ion chromatography describes the analysis of dissolved ions by ion exchange chromatography using electrical conductivity detection.

The methods used in the analysis of the corrosion product included simple gravimetric analysis, thermogravimetric analysis, X-ray fluorescence, and infrared spectroscopy.

The corrosion product appeared to be a low density form of iron rust. Simple gravimetric analysis was performed by measuring the sample weight before and after firing. The difference in the weights of the original sample and the ash, Fe_2O_3, was attributed to water of hydration and organically bound material.

Thermogravimetric analysis was done with a DuPont Instruments model 990 thermal analyzer. This analysis gave more detailed information about the volatile matter in the corrosion products. In the procedure, an oxygen atmosphere was used which oxidized all carbon and hydrogen in the sample to gaseous products and converted the iron to hematite, Fe_2O_3.

The iron content of the corrosion product was measured with an EDAX International model 902 elemental X-ray analyzer. Infrared spectra of the corrosion product were obtained with a Beckman microlab model 620MX spectrometer and a Fourier transform infrared (FTIR) spectrophotometer. Spectra of both the amorphous corrosion products, using the KBr-pellet technique, and the intact surface corrosion product, using attenuated total reflectance, were obtained.

C. Droplet Combustion Products

The purpose of this experiment was to determine the water-soluble combustion intermediates that are present in the diffusion flame envelope that surrounds a burning methanol droplet. In this experiment, methanol droplets were formed by gravity feed through a burette and allowed to fall about 1 meter into a vessel containing about 20 mL of ice cold distilled water. The droplets were ignited by a methane pilot flame placed in the line of fall about 15 cm below the burette. After about 100 burning droplets (ca. 4 mL methanol) were quenched in the water, the resulting aqueous-methanol solution was analyzed for formaldehyde, formic acid, and peroxides. The results given in Table 12 for different numbers of droplets quenched in 20 mL of water show that formaldehyde, formic acid, and peroxides are formed in the burning methanol droplet. Calculations based on the data in Table 12 indicate that each droplet of methanol formed 1.2 mcgm of peroxide, 5.7 mcgm of formaldehyde, and 1.33 mcgm of formic acid. Based on an average droplet diameter of

39

TABLE 12.   COMBUSTION PRODUCT ANALYSIS OF
WATER-QUENCHED METHANOL DROPLETS

No. of Droplets*	pH	Combustion Product Concentrations in ppm		
		Peroxide	Formaldehyde	Formate Ion
50	4.8	3.8	14	3.0
100	4.1	6.0	30	3.9
200	3.9	9.6	48	12.7
300	3.8	13.2	62	15.8

* Burning methanol droplets were captured in 20 mL of deionized ice
water.   One mL of methanol is equivalent to 54 drops.

1.33 mm, the concentrations of peroxide, formaldehyde, and formic acid in the
droplet would be 65, 308, and 72 ppm if it is assumed that the combustion
products are dissolved in the fuel.

It is conceivable that products dissolve in the droplet as it burns and
eventually, as the methanol is depleted, the droplet becomes enriched with
water, formaldehyde, formic acid, and peroxides. Because methanol has a
relatively low boiling point, it tends to evaporate and burn, leaving the
less volatile products in the droplet. In a cold engine, droplet combustion
is prevalent, and it is possible that droplets provide a mechanism for trans-
porting deleterious combustion products to the cylinder wall.

A cast-iron sample was exposed to burning droplets of methanol, and the sur-
face corrosion product was examined using FTIR spectroscopy. The cast iron
sample made from a part of the 2.3-liter engine block was machined to fit the
sample holder of the attenuated total reflectance attachment of the FTIR.
Burning droplets of methanol made in the experiment described above were
intercepted by the cast-iron sample. Sometimes the droplets would impinge on
the sample and continue to burn, forming a flame over the surface. There-
fore, it was not clear which was most important in the corrosion process, (1)
the combustion products carried by the droplets, or (2) the products being

transported from the flame to the liquid methanol film on the surface. In either event, corrosion products forming on the surface were apparent after only a few minutes with a droplet impingement rate of about 30 per minute. Although the surface corrosion appeared to be rust, the attenuated reflectance absorption spectrum (see Figure 8) of the surface showed bands at 3210, 2868, 1572, 1361, and 930 cm^{-1}. The relatively weak bands at 2868 cm^{-1} and 3310 cm^{-1} were characteristic of CH and OH bonds, respectively. The three relatively strong bands remaining were identified as the formate ion. These results agreed with earlier work (29) which showed that the corrosion product was a form of iron formate. Further analysis of the corrosion product using gravimetric analysis and X-ray fluorescence is discussed in another section of this report.

At this stage in the work, the actual combustion intermediates responsible for the corrosion were not yet clearly identified. Qualitative experiments on the reactivities of formaldehyde, formic acid, and hydrogen peroxide showed that none of them individually would cause rapid corrosion of cast iron. However, when different combinations of the combustion products were used, it was found that aqueous solutions of hydrogen peroxide with either formaldehyde or formic acid added, caused vigorous corrosion of cast iron. The reaction of hydrogen peroxide with formaldehyde to form formic acid is relatively slow*, but in the presence of transition metals, such as iron and copper, concentrated solutions of hydrogen peroxide and formaldehyde react rapidly. However, the reaction of hydrogen peroxide and formic acid with iron appeared to cause more corrosion faster, probably because the peroxide was utilized solely in the oxidation of iron. In the following sections on combustion residues and corrosion mechanisms, it becomes clear that corrosion is caused by the peroxide and formic acid.

D. Combustion Residues

The pool-burning experiments were carried out in shallow dish-shaped containers made of cast iron, aluminum, and stainless steel. The containers

---

* The kinetics of this reaction are discussed in the appendix of this report.
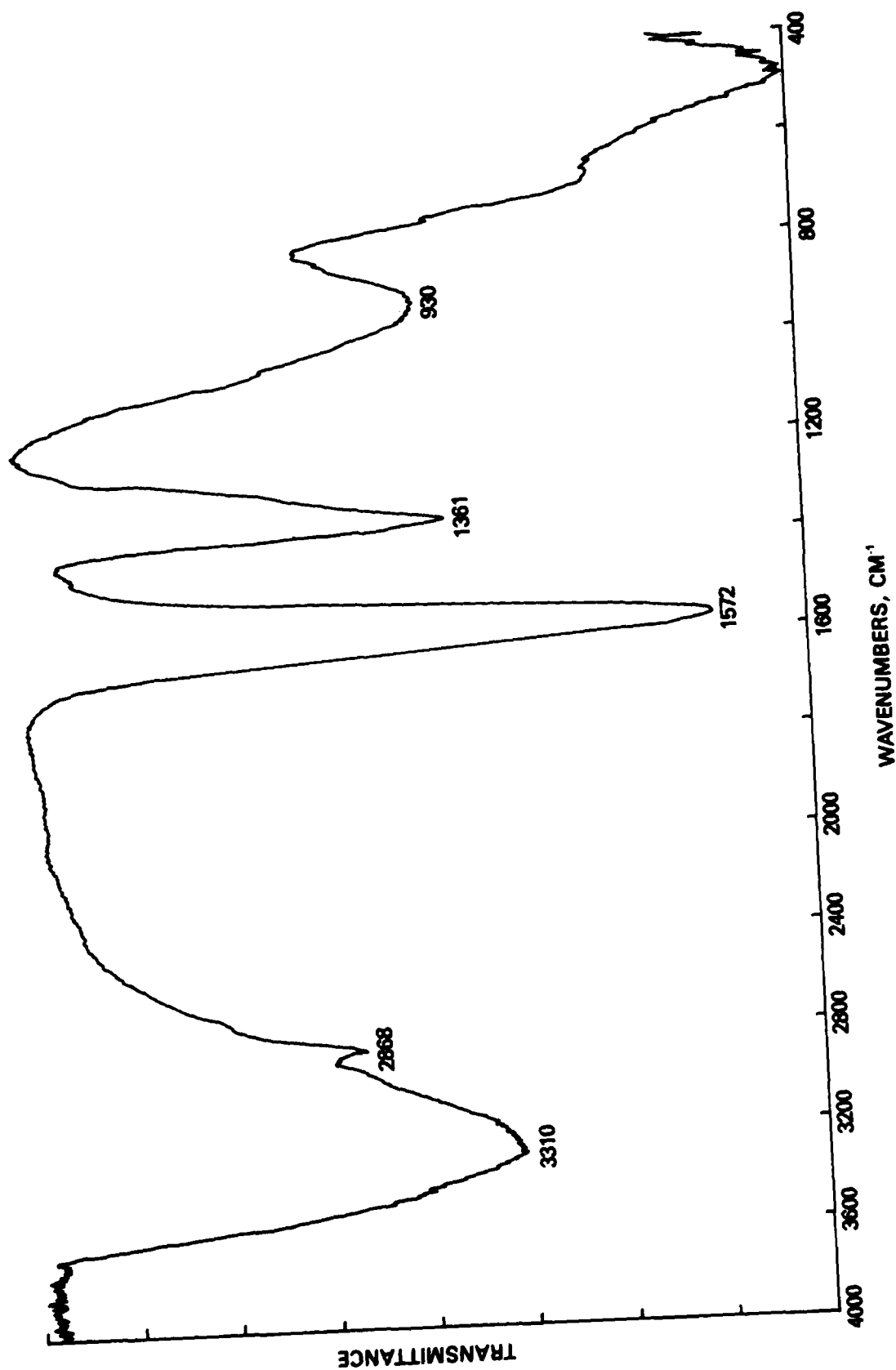
FIGURE 8. ATTENUATED TOTAL REFLECTANCE SPECTRUM OF INTACT SURFACE CORROSION PRODUCT FORMED BY INTERACTION OF BURNING METHANOL DROPLETS WITH CAST IRON

42

were placed in a water bath as shown in Figure 9 to prevent the temperature from increasing too much as the fuel burned. Care was taken to ensure that the initial temperature (22°C) of the water bath was always the same. In a typical experiment, the container was filled to the brim (a depth of 6 mm) with fuel, ignited with a pilot flame, and permitted to burn to the point of extinction. In experiments with neat methanol using tap water (at 22°C) as the coolant, it was found that a liquid residue was left after flame extinction with significant corrosion in the cast-iron container. Figure 10 shows the containers before and after burning neat methanol pools. Although substantial corrosion occurred on the cast-iron container, none was observed in those made of aluminum and stainless steel.

FIGURE 9.   STAINLESS-STEEL CONTAINER FOR POOL-BURNING
EXPERIMENT COOLED IN WATER BATH

CAST IRON

STAINLESS

ALUMINUM

A   B
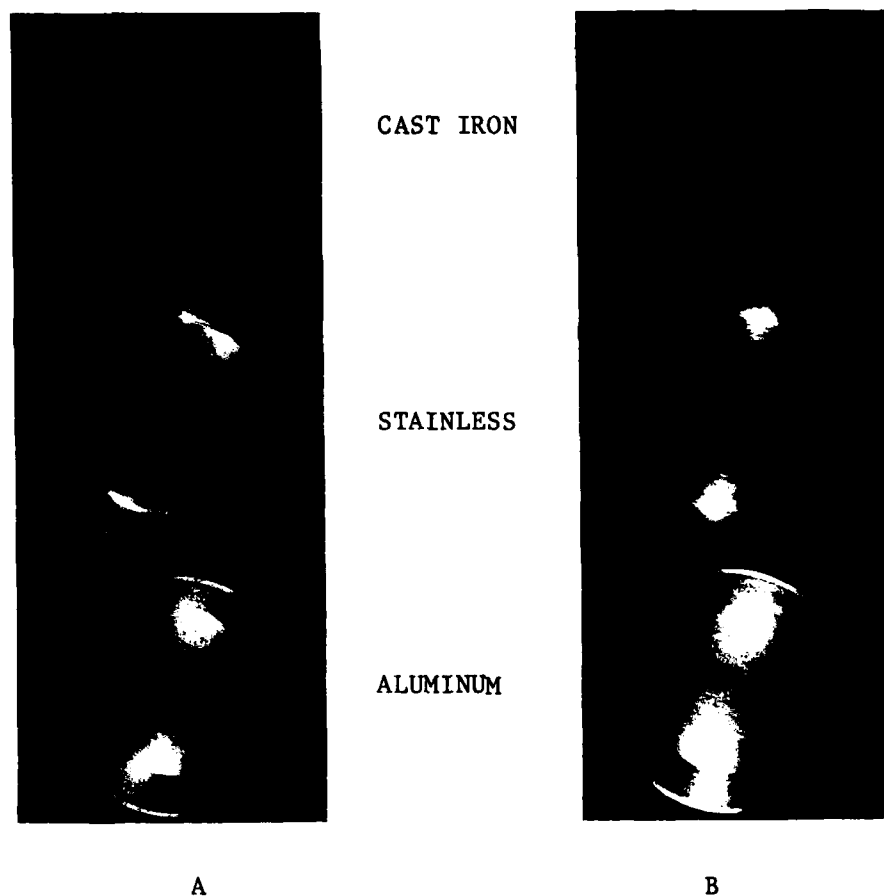
FIGURE 10. CAST IRON, STAINLESS STEEL, AND ALUMINUM CONTAINERS
BEFORE, A, AND AFTER, B, BURNING NEAT METHANOL POOLS

1.   Corrosion Products

To determine the combustion-associated corrosive tendencies of low molecular
weight alcohols, it was necessary to burn the fuel 10 times in the cast-iron
container to make enough corrosion products for a weight measurement. The
liquid residue left in the container after the 10 burns was evaporated in a
vacuum desiccator. The dried corrosion products were scraped from the con-
tainer and placed in a crucible for firing. The weight of the corrosion
product was recorded before and after firing so that the amount of volatile
matter could be determined. Upon firing, it was evident from the smoldering

and sooty appearance of the corrosion product that it was partly composed of organic matter. The inorganic material left in the crucible appeared to be hematite, Fe_2O_3. The weight of Fe_2O_3 was used to gauge the corrosion tendency of the fuel. Figure 11 shows infrared spectra obtained by the KBr-pellet technique of the dried corrosion product and the hematite formed after firing in a crucible. The spectrum of the corrosion product was essentially the same as that obtained for surface deposits in Figure 8 using the FTIR spectrometer. It is clear that none of the absorptions can be attributed to iron oxide. The spectra show that the deposit is different from rust in that it contains OH, C-H, and formate ion ($HCOO^-$) groups. An analysis of the corrosion product using thermogravimetric analysis showed that it contained two volatile components. The measurements were carried out in an oxygen atmosphere to ensure that the iron would be converted to hematite. The first volatile component appeared at about 100°C; the second at about 200°C. The second component was organic because it ignited during the volatilization process. The first component appeared to be water because of its volatilization temperature and the strong OH absorption in the infrared spectrum. The thermogravimetric analysis was not very quantitative because the various samples of the corrosion product showed a high degree of variation in volatile matter. Most of the sample contained at least 30 percent volatile matter, of which 20 percent was organic. Somewhat more quantitative results were obtained from the simple gravimetric analysis of corrosion products. The corrosion products formed by burning neat methanol and methanol containing 10 percent water were weighed, fired, and weighed again so the weight loss could be determined. The weight loss for the corrosion product from neat methanol averaged 31.8 ± 1.9 percent; the methanol/water blend weight loss averaged 39.9 ± 1.8 percent. These average weight losses were each based on the analysis of seven samples. It appeared that the difference between the two corrosion products was in the amounts of hydrated water. The strength of the OH infrared absorption band varied significantly among the samples, indicating that their water contents were quite variable. Based on the weight loss data from the gravimetric measurements and the infrared spectra, it was concluded that the 31.8 percent weight loss corresponded with the empirical formula FeO(HCOO) while the 39.8 percent weight loss corresponded with $FeO(H_2O)(HCOO)$.
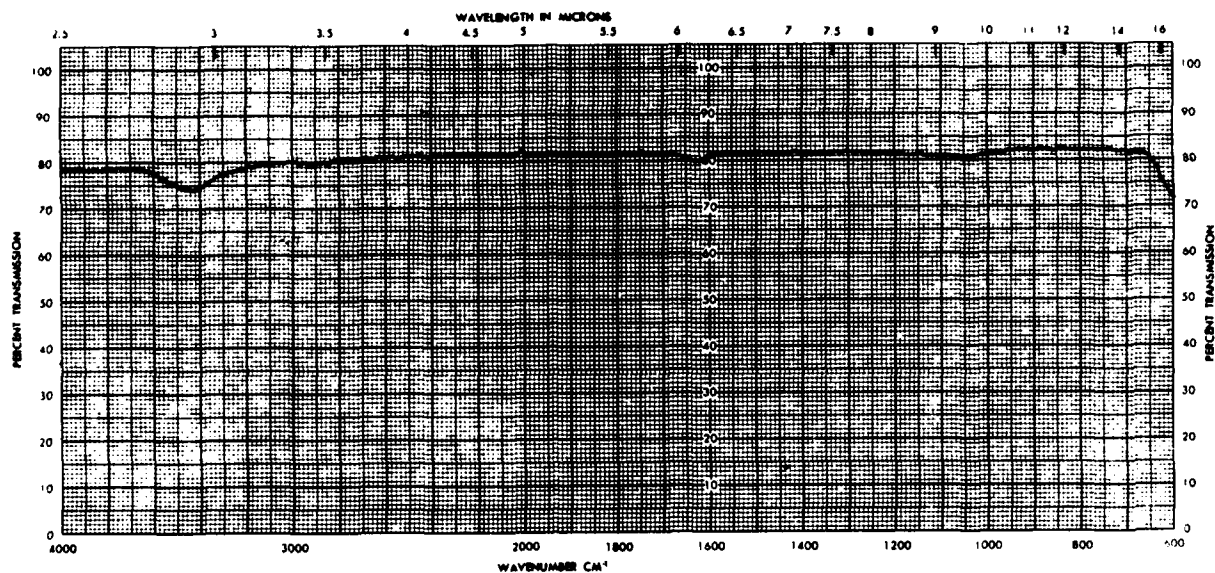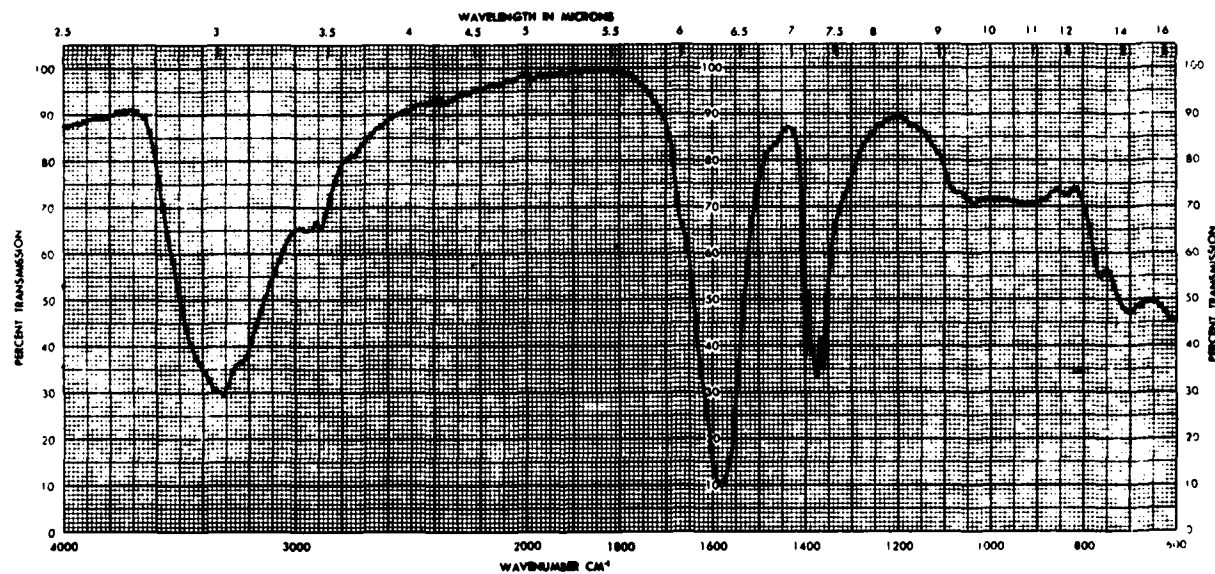
FIGURE 11. INFRARED SPECTRA OF IRON OXIDE (Fe_2O_3), A, AND
CORROSION PRODUCT, B, OBTAINED BY THE KBr-PELLET TECHNIQUE

2. Combustion Residue Volume

Experiments were then carried out to determine the amounts of liquid combustion residue left in the containers after burning various fuels. It was important in these experiments to remove the residue as soon as possible after flame extinction to prevent loss by evaporation. The measurements were done in triplicate, and care was taken to use a consistent technique. Table 13 shows the residue volumes and the relative corrosion tendencies (mg Fe_2O_3) of several fuels based on the Fe_2O_3 formed when the fuel was burned in the cast iron containers. The results showed that the corrosion tendencies and the residue volumes were the highest among the methanol-containing fuels and decrease as the molecular weight of the alcohol increased. The most striking result was the comparison of methanol with isooctane. Note that the residue volume for neat ethanol in Table 13 is listed as zero; this does not mean that there was absolutely no residue formed. Actually, some residue appeared when neat ethanol was burned, but it evaporated within seconds after the flame extinguished. Significant increases in both residue volume and corrosion occurred when the fuel contained water. The volatility additive methylal (dimethoxymethylene) in methanol had little or no effect on the residue volume or the extent of corrosion. As a whole, the results showed that corrosion tendency correlated strongly with the tendency to form a combustion residue. This is apparently the reason why methanol causes more cylinder bore and ring wear than ethanol. In the engine tests using methanol/11 percent water and ethanol/11 percent water, the wear rates increased dramatically above those for the neat alcohol fuels. These relative wear rates correlated quite favorably with the combustion residue volumes shown in Table 13.

3. Temperature Effects

It was found that the amount of combustion residue remaining after flame extinction depended on the temperature of the container. The effect of coolant temperature on residue volume was measured in the apparatus shown in Figure 12. This apparatus (3 in. dia. x 3/8 in. deep) was specifically designed for the study of pool burning work in a different program at a date

47

TABLE 13. COMBUSTION RESIDUE VOLUMES AND RELATIVE CORROSION
TENDENCIES BASED ON Fe_2O_3 FORMED

| Fuel | Residue Volumes* (mL) | | | Fe_2O_3 |
	Cast-Iron Container	Aluminum Container	Stainless-Steel Container	Cast-Iron Container
Neat Methanol	0.33	0.13	0.37	12.5
Neat Ethanol	0.0	0.0	0.0	10.8
Neat Isopropanol	0.0	0.0	0.0	0.6
Methanol/10% Methylal	0.33	0.19	0.43	--
Methanol/10% Water	1.63	0.93	2.06	26.6
Ethanol/10% Water	0.42	0.35	0.39	22.7
Isopropanol/10% Water	0.12	0.21	0.06	15.6
Isooctane	0.0	0.0	0.0	0.0

The container volumes were: Cast iron (13.5 mL), aluminum (13.6 mL),
stainless steel (19.0 mL).
* Analyses are based on three runs.

well after most of the experimental work was completed in this program. The
apparatus was particularly useful in examining the effects of coolant temper-
ature on combustion residue volume. The temperature of the coolant passing
through the vessel was controlled by simply varying the relative amounts of
hot and cold tap water available in the laboratory facility. A thermocouple
and digital readout was used to measure the coolant temperature in the appa-
ratus.

Neat methanol was burned in the apparatus at several temperatures ranging
from 22° to 50°C. In each run, 40 mL of neat methanol were burned to extinc-
tion in the apparatus, and the residue was collected and weighed. Figure 13
shows that the residue weight decreased linearly with increasing coolant
temperature. The results indicated that residue should cease to be present
when the coolant temperature is above 58°C. However, this is not to say that
deleterious combustion products dissolved in the methanol and present in the
liquid fuel just prior to flame extinction would not cause corrosion of metal
surfaces for a finite period of time.
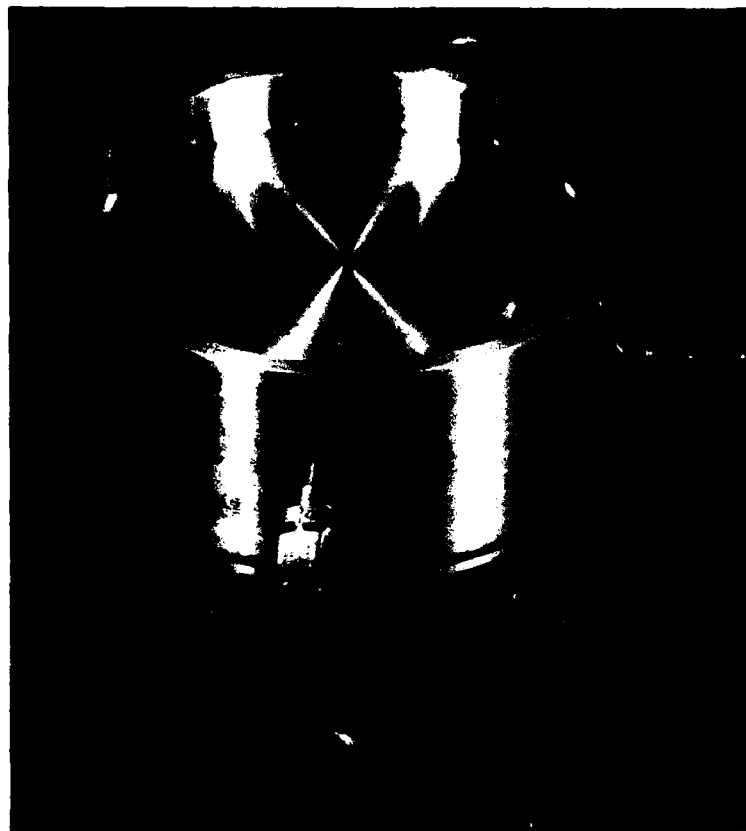
FIGURE 12.   SHALLOW POOL BURNING APPARATUS

It is clear from the shape of the curve shown in Figure 13 that the tempera-
ture dependence of the residue weight is quite different from the exponential
dependence of wear metals buildup shown earlier in Figure 3.   It was con-
cluded earlier that the wear rate depended on the time required for the
evaporation of liquid methanol from the cylinder wall.   Note that both the
wear rate and the calculated evaporation rate had the same temperature depen-
dence.   This temperature dependence indicated that they were related phenom-
ena.   Since the temperature dependencies of the wear rate and the residue
weight were distinctly different, it appeared that the formation of the
combustion residue was a secondary process, whereas the primary process
responsible for the observed temperature dependence of the wear was the rate
of evaporation of liquid from the cylinder wall.

$R = 24.8 - 0.0749T$

$R^2 = 0.947$
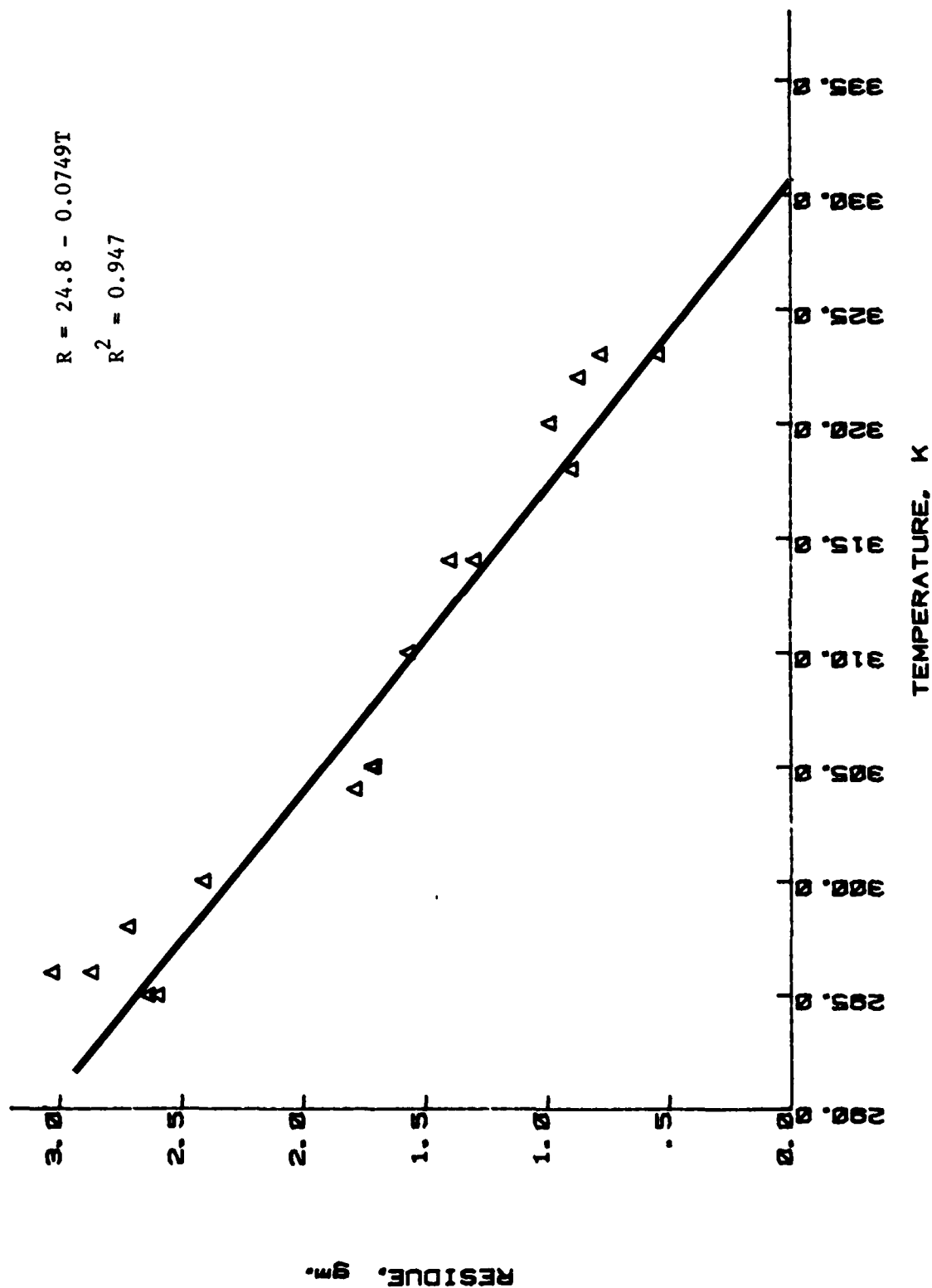
FIGURE 13. CORRELATION OF RESIDUE VOLUME
WITH FUEL TEMPERATURE AT FLAME EXTINCTION

50

4. Combustion Residue Composition

Chemical analysis of the residues obtained from a methanol/10 percent water mixture burning in cast iron, aluminum, and stainless-steel containers is given in Table 14. While the major components of the residues were water and methanol, there were significant quantities of formaldehyde, formic acid, and peroxide. The concentrations of formaldehyde and formate ion in the residues were about the same in all three containers. In the corrosion-resistant aluminum and stainless-steel containers, the concentrations of formic acid and peroxide were similar, but there was no trace of these species in the residue formed in the cast-iron dish. Instead, the residue from the cast-iron dish contained formaldehyde, formate ion, and iron, and its pH increased significantly. These results showed that the iron formate was produced by the reaction of formic acid and peroxide with cast iron. The other possible reaction of peroxide and formaldehyde with iron mentioned earlier appeared to be unimportant in this corrosion process.

TABLE 14. METHANOL/10 PERCENT WATER COMBUSTION RESIDUE ANALYSIS

Fuel	Cast-Iron Container	Aluminum Container	Stainless-Steel Container
Water, wt%	76	76	77
Methanol, wt%	23	23	22
Formaldehyde, ppm (mg)	14021 (22.9)	15049 (14.0)	14195 (29.4)
Peroxide, ppm (mcg)	0	879 (818)	1005 (2080)
Formic Acid, ppm (mcg)	0	2581 (2400)	2923 (6050)
Formate, ppm (mcg)	2130 (3472)	1980 (1841)	2450 (5072)
Iron, ppm (mcg)	1070 (1744)	0	0
pH	4.9	--	2.6
Formic Acid Calc*, ppm	0.04	--	1649
Dish Volume, mL	13.5	13.6	19.0
Residue Volume, mL	1.63	0.93	2.07

Analysis are based on three runs.
*Calculated from pH

The chemical analysis of residues from neat methanol, methanol/10 percent methylal, ethanol/10 percent water, and isopropanol/10 percent water are given in Tables 15 through 18. The formic acid concentrations in these residues were not measured by gas chromatography; they were calculated from the pH of the residue. When the residues were formed in the relatively inert stainless-steel container, the formic acid concentrations calculated from pH were similar to the formate ion concentrations measured by ion chromatography. The formate ion concentrations were higher than the formic acid concentrations calculated from pH because residues contained some alcohol which raises the pH.

The chemical compositions of the residues from neat methanol and methanol containing the volatility additive, methylal, were essentially the same. Compared to the methanol/10 percent H_2O residue, the concentrations of both combustion products and corrosion products in the neat methanol residues were higher. Note that, on the other hand, the residue volumes obtained in the

TABLE 15. NEAT METHANOL COMBUSTION RESIDUE ANALYSIS

Fuel	Cast-Iron Container	Aluminum Container	Stainless-Steel Container
Water, wt%	75	74	76
Methanol, wt%	23	23	22
Formaldehyde, ppm (mg)	2.08 (6.86)	2.45 (3.19)	2.18 (8.07)
Peroxide, ppm (mcg)	0	3133 (407)	5235 (1937)
Formate, ppm (mcg)	4550 (1501)	3338 (434)	6677 (2470)
Iron, ppm (mcg)	2460 (812)	0	0
pH	4.8	--	2.39
Formic Acid Calc*, ppm	0.06	--	4329
Dish Volume, mL	13.5	13.6	19.0
Residue Volume, mL	0.33	0.13	0.37

Analyses are based on three runs.
*Calculated from pH.

TABLE 16. METHANOL/10 PERCENT METHYLAL COMBUSTION RESIDUE ANALYSIS

Fuel	Cast-Iron Container	Aluminum Container	Stainless-Steel Container
Water, wt%	75	74	76
Methanol, wt%	23	22	22
Formaldehyde, ppm (mg)	2.25 (7.43)	2.04 (6.73)	2.02 (8.69)
Peroxide, ppm (mcg)	0	2773 (527)	5177 (2226)
Formate, ppm (mcg)	4900 (1617)	3596 (683)	5615 (2414)
Iron, ppm (mcg)	2020 (667)	0	0
pH	4.8	--	2.4
Formic Acid Calc*, ppm	0.06	--	4142
Dish Volume, mL	13.5	13.6	19.0
Residue Volume, mL	0.33	0.19	0.43

Analyses are based on three runs.
* Calculated from pH.

TABLE 17. ETHANOL/10 PERCENT WATER COMBUSTION RESIDUE ANALYSIS

Fuel	Cast-Iron Container	Aluminum Container	Stainless-Steel Container
Water, wt%	75	74	76
Ethanol, wt%	23	23	22
Formaldehyde, ppm (mg)	0.391 (1.64)	0.368 (1.29)	0.403 (1.57)
Peroxide, ppm (mcg)	0	4101 (1435)	6046 (2358)
Formate, ppm (mcg)	1000 (420)	811 (284)	1102 (430)
Iron, ppm (mcg)	2015 (846)	0	0
pH	5.0	--	3.11
Formic Acid Calc*, ppm	0.02	--	157
Dish Volume, mL	13.5	13.6	19.0
Residue Volume, mL	0.42	0.35	0.39

Analyses are based on three runs.
* Calculated from pH.

TABLE 18.— ISOPROPANOL/10 PERCENT WATER COMBUSTION RESIDUE ANALYSIS

Fuel	Cast-Iron Container	Aluminum Container	Stainless-Steel Container
Formaldehyde, ppm (mg)	0.130 (0.16)	0.110 (0.23)	0.199 (0.11)
Peroxide, ppm (mcg)	0	4616 (969)	15608 (884)
Formate, ppm (mcg)	562 (69)	485 (102)	1376 (78)
Iron, ppm (mcg)	10833 (1300)	0	0
pH	4.9	3.5	2.81
Formic Acid Calc*, ppm	0.03	13	277
Dish Volume, mL	13.5	13.6	19.0
Residue Volume, mL	0.12	0.21	0.06

Analyses are based on three runs.
* Calculated from pH.

neat methanol fuel were much lower than those from the methanol/10 percent water blend. The combustion products appeared to be more concentrated in the neat methanol residue because the residue volume was much lower than that obtained from the methanol/10 percent water blend.

On a weight basis, neat methanol residues contained less formaldehyde and formic acid than the methanol/10 percent water residue, but the amounts of peroxide were similar. Also, results in Tables 14, 17, and 18 show that amounts of formaldehyde and formic acid decreased as the molecular weight of the alcohol increased. However, the concentrations of peroxide were similar in magnitude for all the alcohols. It was also interesting to note that the ratios of formaldehyde to formic acid (formate ion) in the combustion residues formed from the 10 percent water blends with methanol, ethanol, and isopropanol are 6.7, 4.0, and 2.0, respectively. The following section on pool-burning history helps to explain these results.

5. Pool-Burning History

Experiments were carried out to determine the history of liquid phase buildup of combustion products in burning pools of neat methanol and neat ethanol. The fuels were burned for different periods of time in a stainless-steel container cooled with tap water as shown in Figure 9. In a typical experiment, the stainless-steel container was filled with fuel, ignited, and after a given burning time, smothered. A sample of the unburned fuel was retained for analysis, and the container was refilled with fresh fuel for the next burn. Samples of the unburned fuel were collected at burning times ranging from 1.0 to 6.0 minutes; flame extinction occurred at about 6.5 minutes.

Figures 14 and 15 show the buildup in the concentrations of combustion products as the fuel was consumed. Figures 16 and 17 show the net mass accumulation of combustion products in the fuel as it was burned. While the concentrations of combustion products in the fuel increased continuously as the fuel burned, the net mass accumulations tended to decrease when most of the fuel was consumed. The net mass accumulation rates were positive for most of the burning period, but turned negative at the end, indicating a net loss of products due to evaporation near the time of flame extinguishment. Based on the fuel consumptions when the net mass accumulation rates became negative, Figures 16 and 17 show that the relative volatilities of combustion products decreased in order, water > formaldehyde > formic acid > peroxide. Since the peroxide and formic acid were the least volatile species, they would tend to become highly concentrated on the surface of a cylinder wall as the combustion residue evaporated. This would obviously lead to corrosion of an unprotected iron surface.

As noted earlier, the concentrations of formaldehyde and formic acid in the combustion residues from the ethanol/10 percent water blend and, especially the isopropanol/10 percent water blend, were much smaller than those found in the methanol/10 percent water blend. Although chemistry determines to a great extent the concentrations of formaldehyde and formic acid in the combustion residues, evaporation is also very important. Evaporation decreases both the combustion residue volume and the ratio of formaldehyde to formic acid as the molecular weight of the alcohol is increased.

55

FIGURE 14.   BUILDUP IN THE CONCENTRATIONS OF COMBUSTION PRODUCTS
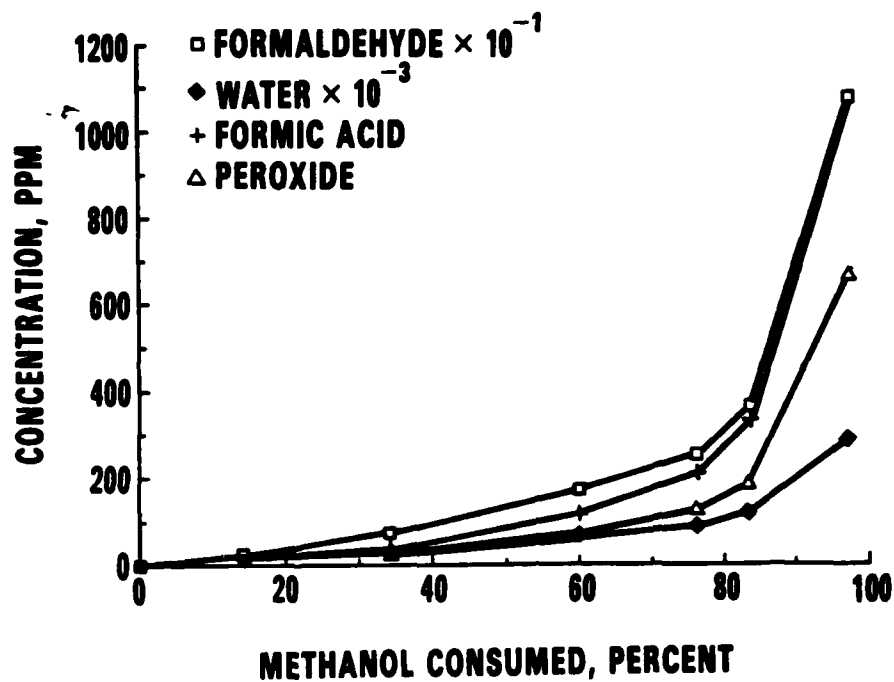IN THE LIQUID PHASE OF A BURNING METHANOL POOL
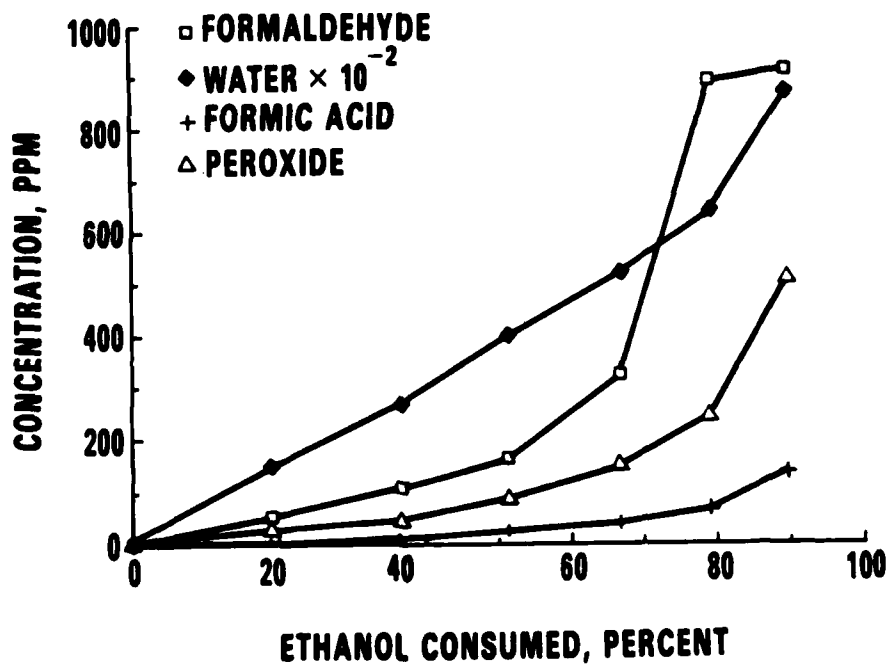
FIGURE 15.   BUILDUP IN THE CONCENTRATIONS OF COMBUSTION PRODUCTS
IN THE LIQUID PHASE OF A BURNING ETHANOL POOL

56
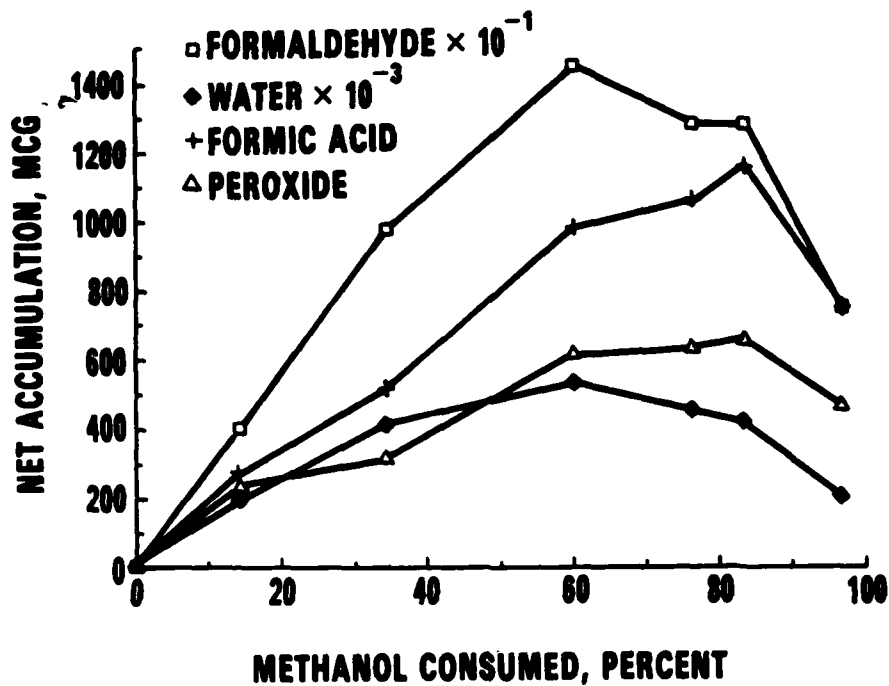
FIGURE 16.   NET MASS ACCUMULATIONS OF COMBUSTION PRODUCTS
IN LIQUID PHASE OF A BURNING METHANOL POOL
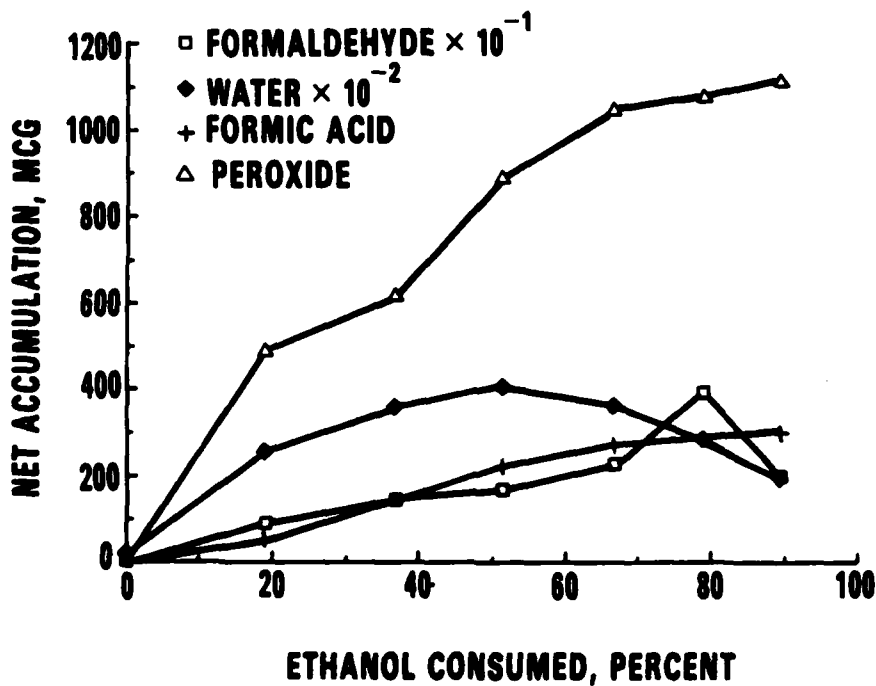
FIGURE 17.   NET MASS ACCUMULATIONS OF COMBUSTION PRODUCTS
IN LIQUID PHASE OF A BURNING ETHANOL POOL

57

Isopropanol and ethanol have higher heating values than methanol, and their flames are also more luminous so heat transfer back to the fuel pool increases the temperature and the evaporation rate. The average burning times for methanol, ethanol, and isopropanol fuels containing 10 percent water were 6.5, 7.3, and 7.5 minutes, and the heating values in kcal/mL were 3.82, 5.06, and 5.59 respectively. The relative heat release rates for the methanol, ethanol, and isopropanol fuels turned out to be 1.00, 1.18, and 1.27, respectively. This appears to be one of the important reasons why residue volume decreased as the molecular weight of the alcohol increased. Another factor was the solubility of combustion products in the alcohol. It is well known that the solubility of oxygenates, including water, decreases as the molecular weight of the alcohol is increased. The boiling point of the alcohol also played a role. When the boiling point of the alcohol is low compared to water, the alcohol evaporates almost exclusively, leaving the aqueous solution of combustion products behind. When the boiling points of the alcohol and water are similar, as is the case with isopropanol, the water tends to evaporate along with the alcohol.

E.   Corrosion Chemistry

It was concluded earlier that corrosion of iron by the methanol fuel residues was caused by formic acid and peroxide. However, the importance of formic acid versus peroxide in the mechanism has not been discussed. The amount of iron dissolved from the cast-iron container when the methanol was burned seems to be easily accounted for by the amounts of peroxide and formic acid in the residue. Thus, the moles of peroxide were sufficient to oxidize the iron, and there was more than enough formate ion to combine with all the iron ions.

The concentrations of formic acid (formate ion) in the ethanol/10 percent water and the isopropanol/10 percent water combustion residues were much lower than that found in the methanol residue, but the peroxide concentrations were similar in all the combustion residues. Since the concentrations of iron in the residues formed in the cast-iron container appeared to parallel the peroxide concentration, it became apparent that the peroxide must also play an important role in the corrosion process.

There are three possible mechanisms for the corrosion of iron by formic acid. The first is the simple displacement of hydrogen by iron.

$$Fe^\circ + 2HCOOH = Fe^{++} (HCOO^-)_2 + H_2$$

In this oxidation-reduction reaction, iron displaces hydrogen because it is above hydrogen in the electromotive series of elements.[30] The second mechanism for the corrosion of iron is well known as "rusting;" it occurs when iron is in the presence of oxygen, water, and an electrolyte.[31] To understand this mechanism, it is helpful to envision a multitude of cathodes and anodes arbitrarily assigned to the surface of the metal. Oxygen is reduced at the cathode

$$O_2 + H_2O + 2 \text{ electrons} = 2OH^-$$

and iron is oxidized at the anode.

$$Fe^\circ - 2 \text{ electrons} = Fe^{++}$$
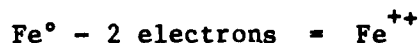
This corrosion process will not occur unless an electrolyte such as formic acid is present. When formic acid is the electrolyte, the OH^- ions combine with H^+ ions to make water, and Fe^{++} ions combine with $HCOO^-$ ions to make iron formate. As the corrosion process proceeds, the H^+ ions are consumed and the pH increases.

The third mechanism is essentially the same as the second except a peroxide takes the place of O_2. In this case, the cathode reaction

$$R_2O_2 + 2 \text{ electrons} = 2RO^-$$

is expected to be faster than the analogous reaction with O_2. The peroxide, R_2O_2, present in combustion residues appears to be dioxymethylene peroxide which is formed by the reaction of hydrogen peroxide with formaldehyde. R is the methylene hydroxy radical (CH_2OH). This is covered in the appendix of this report.

Corrosion Experiment - To determine the effects of formic acid and peroxide on the corrosion process, an experiment was carried out to measure the rate of iron dissolution by combustion residues. The combustion residues were prepared by blending water, methanol, formaldehyde, formic acid, and hydrogen peroxide in the proportions typically found in the methanol combustion residue. The experiment was performed in the apparatus shown in Figure 18. An iron strip was placed in a 100-mL beaker containing 20 mL of the synthetic residue. The residue solution was stirred so that a consistent concentration gradient would be developed at the liquid-metal interface. The beaker containing the residue was placed in a water bath (see Figure 18) to help stabilize the temperature, which was controlled by simply balancing the heat loss from the water bath with the heat input from the hot plate. The iron strip was exposed to the residues for durations ranging from 0.5 to 5.0

FIGURE 18. APPARATUS USED TO MEASURE IRON DISSOLUTION
BY COMBUSTION RESIDUES

minutes and temperatures ranging from 23° to 54°C. After each exposure of the iron strip to the residue, the contents of the residue were analyzed for iron by atomic absorption spectroscopy. Three synthetic residue compositions were made by adding either formic acid or hydrogen peroxide or both to a base residue blend containing about 74 vol% water, 24 vol% methanol, and 1.5 vol% formaldehyde. The concentration of formic acid, added to reach a pH of 2.6, was about 2500 ppm. In residues containing hydrogen peroxide, a concentration of 1200 ppm was used. Because hydrogen peroxide reacts slowly at room temperature with formaldehyde to form formic acid, the residue composed of base material and hydrogen peroxide was prepared just prior to use in the experiment. Figure 19 shows the buildup of dissolved iron versus time at 42°C for different residue compositions. The data included in Figure 19, as well as that obtained at other temperatures, is given in Table 19. The results showed that both formic acid and peroxide were important in the corrosion mechanism. Iron dissolved at a moderate rate when only formic acid was
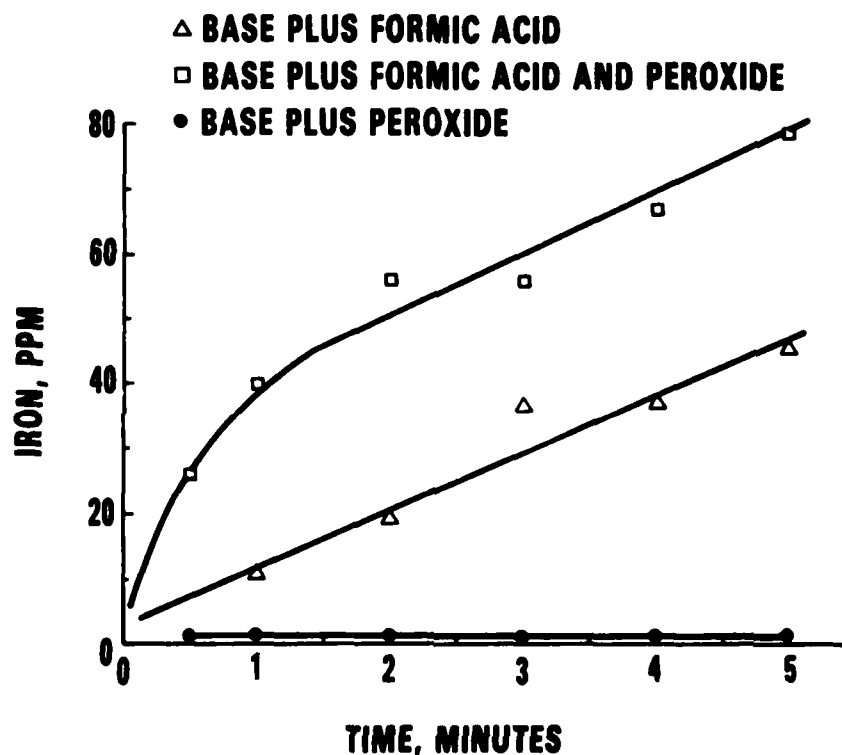
FIGURE 19. THE EFFECTS OF FORMIC ACID AND PEROXIDE ON THE DIS-
SOLUTION OF IRON BY SYNTHETIC METHANOL COMBUSTION RESIDUES

61

TABLE 19. DISSOLUTION OF IRON BY
SYNTHETIC COMBUSTION RESIDUES

Residue*	Reaction Time, min	Temperature, °C	Iron Buildup, ppm
A	1.0	23	13
B	1.0	23	30
A	1.0	37	11
B	1.0	37	39
A	1.0	54	7
B	1.0	54	46
B	0.5	45	26
C	0.5	45	0.1
A	1.0	45	11
B	1.0	45	40
C	1.0	45	0.2
A	2.0	45	20
B	2.0	45	56
C	2.0	45	0.3
A	3.0	45	37
B	3.0	45	56
C	3.0	45	0.3
A	4.0	45	38
B	4.0	45	67
C	4.0	45	0.3
A	5.0	45	46
B	5.0	45	79
C	5.0	45	0.4

* The combustion residue A is a mixture of water, methanol, formaldehyde
in weight proportions of 75:23:1.5 with formic acid added to lower the pH
to 2.6. Residue B was prepared by adding 1200 ppm of hydrogen peroxide
to residue A. Residue C was the same as B, except that it did not con-
tain formic acid.

present in the base residue blend, but when hydrogen peroxide was added, the
initial rate of dissolution was substantially increased. The residue con-
taining only peroxide was not at all effective in dissolving iron. It is
interesting to note that iron dissolution by residue composition A in
Table 19 decreased as the temperature was increased. The dissolution rate
appeared to decrease with increasing temperature because the amount of dis-
solved oxygen was reduced as the residue was heated. When real combustion
residues are formed from burning pools of alcohol, or for that matter on a

cylinder wall, the liquid fuel is shielded from oxygen in the combustion chamber. Oxygen was consumed, for the most part, in the combustion process so its concentration was very low at the liquid-gas interface. Also, the solubility of oxygen was relatively low because the temperature at the interface was near the boiling point of the fuel. Since oxidation plays an important role in corrosion, the peroxide found in combustion residues no doubt enhanced the process.

F. Corrosion Test Development

In the final phase of this work, an attempt was made to develop a simple method of testing the effects of fuel additives on iron corrosion by alcohol combustion residues. Several small-scale experiments involving burning pools of alcohol in a cast-iron container were carried out to develop a meaningful test.

In the first test method, the cast-iron container was filled with fuel, ignited, and allowed to burn until all the fuel was consumed. In most cases, it was apparent that some corrosion had occurred, but the actual weight of corrosion product was not very substantial. The partially corroded container was filled with fuel again and burned to completion. This was repeated ten times in order to cause a significant buildup of corrosion product in the container. The container was heated on a hot plate to drive off any volatile residue left in the container. The corrosion product was removed from the container by scraping with a spatula and placing it in a crucible. The crucible was fired, and the amount of Fe_2O_3 in the corrosion product was determined by weight differences. Table 20 shows the corrosive tendencies of fuel in terms of the amount of Fe_2O_3 found after firing the corrosion product. The results are consistent with those mentioned earlier in this report, i.e., the corrosion tendencies of the alcohols decreased with increasing molecular weight. Adding water to the alcohol caused a marked increase in the corrosion tendency, which supports the electrolytic corrosion mechanism discussed earlier.

Basically, additives were chosen for their ability to neutralize formic acid and to reduce peroxides. N,N' disecondary butyl para-phenylene-diamine was

TABLE 20. RELATIVE CORROSION TENDENCIES BASED ON
Fe_2O_3 FORMATION

Fuel Consumption	Fe_2O_3 (mg)
Methanol	12.5
Ethanol	10.8
Isopropanol	0.6
Isooctane	0.0
Methanol + (250 ppm) N,N' disecondary butyl para-phenylene diamine	18.9
Methanol + 10% H_2O	26.7
Ethanol + 10% H_2O	22.7
Isopropanol + 10% H_2O	15.6
Methanol + 10% H_2O + 0.6% Hydrazine hydrate	10.0
Methanol + 10% H_2O + 0.12% Hydrazine hydrate	27.4
Methanol + 10% H_2O + 210 ppm hydroquinone	18.9
Methanol + 10% H_2O + 210 ppm hydroquinone	16.1
Nitromethane	13.8

tested in methanol because it is commonly used as an antioxidant to increase the storage stability of gasoline. The fact that it actually increased the corrosion suggested that it behaved as a chelating agent rather than an antioxidant. Its function in gasoline is not to neutralize peroxides as much as to act as a free radical scavenger. Hydrazine was tried because it is both a base and a strong reducing agent. It seemed to have some beneficial effect at higher concentrations (0.6 percent), but was essentially ineffective at lower concentrations. It was apparent that the hydrazine reacted with formaldehyde because the residue was a white milky substance. It was found later that the same substance could be made by reacting formaldehyde with hydrazine. Hydroquinone, which is an antioxidant, tended to decrease corrosion in

this test. Nitromethane caused about the same amount of corrosion as neat methanol. If the oxides of nitrogen NO, NO_2, HNO_3, etc. are important in real engine wear with methanol fuel, it might be expected that nitromethane would have a greater corrosion tendency than neat methanol. Apparently, significant amounts of nitric acid did not form in the combustion residue.

A second test method was used to determine the effects of fuel type, water content, acids, bases, and reducing agents on the corrosion tendency. In that test, the fuel was burned three times in a cast-iron dish, and the residues were collected as follows. After each burn, one mL of acidic water (pH = 2) was added to the residue in the dish. The acidic water was a very dilute sulfuric acid solution. The contents of the dish were then placed in a 10-mL volumetric flask. The second burn was carried out the same way as the first. After the third and last burn, the dish was rinsed with the acidic water, 2 mL at a time, and added to the volumetric flask until the flask was filled to 10 mL. In several of the tests, some of the iron in the volumetric flask was insoluble. The insoluble portion was brought into solution by adding a single drop of sulfuric acid. The iron content of the solution was then determined by X-ray fluorescence, and ion chromatography was used to measure the formate ion concentration.

Table 21 describes the test fuel and gives the concentration of iron in the diluted residues. The results shown in Table 21 indicate that the presence of water and acid in the fuel increased the rate of corrosion. The water provided a better medium for the reaction and increased the solubility of iron salts formed in the oxidation process. Acids increased the solubility of the corrosion product and tended to keep the iron surface free for subsequent oxidation by peroxide. Making the fuel alkaline by adding a weak base such as ammonium hydroxide may be beneficial in neutralizing formic acid and thereby reducing the solubility of oxidized iron. The results show that a strong base such as sodium hydroxide increased the solubility of oxidized iron. Perhaps this was caused by the somewhat amphoteric nature of iron.

Three reducing agents, hydroquinone, sodium thiosulfate, and ascorbic acid, were used in an attempt to neutralize the peroxide before it reacted with

65

TABLE 21.   IRON CONTENT OF VARIOUS TEST FUEL SOLUTIONS

Test Fuel Description	Iron (ppm)	Formate (ppm)
1. Neat Methanol	246	390
2. Neat Ethanol	139	78
3. Methanol/10% water	306	275
4. Ethanol/10% water	316	155
5. Isopropanol/10% water	130	44
6. Methanol/10% methylal	202	240
7. Neat Acetone	203	70
8. Methanol/nitric acid to make pH = 1.2	485	485
9. Methanol/ammonium hydroxide to make pH = 11.0	207	535
10. Methanol/hydroquinone (640 ppm)	388	430
11. *Methanol/formic acid to make pH = (3.2)	839	1660
12. Methanol/sodium thiosulfate (484 ppm)	334	350
13. Methanol/sodium hydroxide to make pH = 11.6	367	495
14. Methanol/ascorbic acid (754 ppm) to make pH = 5.0	569	880

* By the time the fuel was burned, the methylformate ester had formed and the pH of the fuel was 3.8.

iron. Obviously all attempts failed since the extent of corrosion was greater than that for neat methanol. The sodium thiosulfate seemed to undergo an oxidation reduction type disproportionation reaction forming both sulfide and sulfate. The iron surface became coated with an insoluble black substance that appeared to be iron sulfide. There was no indication that the thiosulfate reduced the peroxide.

Hydroquinone and ascorbic acid would at first glance appear to be good reducing agents for peroxides. It is well-known that ascorbic acid is very effective in reducing ferric ions to ferrous in fruits and vegetables. From the appearance of the combustion residue obtained with methanol/ascorbic acid

fuel, it was evident that the ferric ions (rust colored) were reduced to ferrous ions (clear solution). However, it appeared that the ascorbic acid had little or no effect on the oxidation of neutral iron to the ferrous state. A reasonable explanation for the higher corrosion tendencies indicated by this test procedure is that both hydroquinone and ascorbic acid were weak acids and tended to act as chelates which increased the solubility of iron formate on the surface of the metal.

Figure 20 shows the effect of formate ion concentration on the amount of iron in solution. The numbered data points correspond with the fuel compositions shown in Table 21. The results depicted in Figure 20 indicated that the corrosion product was iron formate. Fuels such as acetone, ethanol, and iso-propanol cause less corrosion than methanol because less formic acid is formed in the combustion process. Acids such as HNO_3 and HCOOH increase the solubility of iron by providing more anions. They also increase the poten-
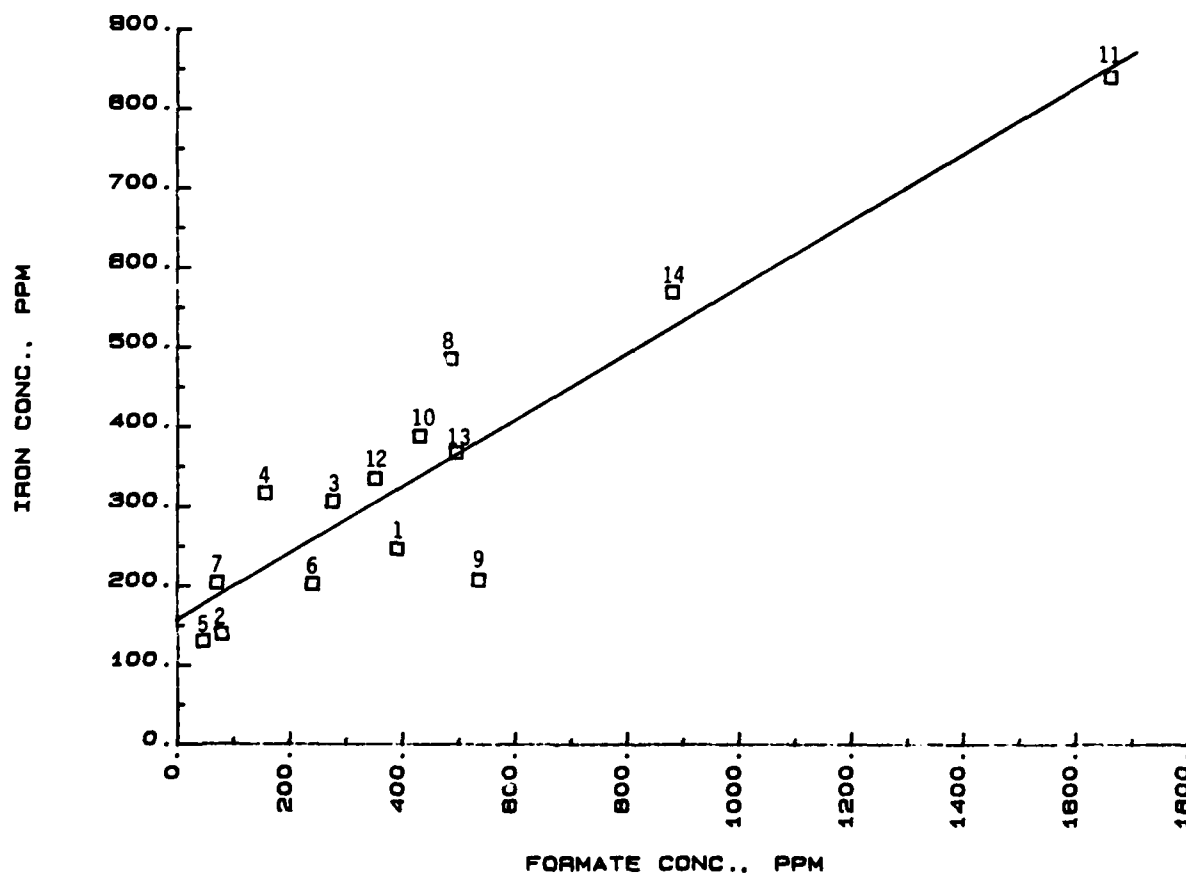
FIGURE 20. DEPENDENCE OF IRON CONCENTRATION ON FORMATE
CONCENTRATION IN COMBUSTION RESIDUES FORMED FROM
BURNING IN A CAST-IRON CONTAINER

67

tial for oxidation by freeing the metal surface of iron oxide. On the other hand, ammonium hydroxide decreased the corrosion rate by rendering iron formate less soluble and base metal less accessible to oxidants.

Other corrosion test methods were developed which were similar to those above and produced basically the same results. In these tests, hydrogen peroxide was also included as one of the fuel additives. It was found that the corrosion tendency of methanol increased significantly when hydrogen peroxide was added to the fuel in concentrations of about 300 ppm. The results were in agreement with work mentioned earlier in this report on the dissolution of iron by combustion residue compositions.

VI. CONCLUSIONS

Several experimental approaches were used to investigate the corrosive nature of the combustion products of low molecular weight alcohols. Combustion residues from burning pools of alcohols were found to contain water, alcohol, formaldehyde, formic acid, and peroxide. The quenching of burning methanol droplets also showed that formaldehyde, formic acid, and peroxide were formed. Combustion residues formed in a cast-iron container caused considerable corrosion of the metal; those formed in aluminum and stainless-steel containers did not cause any corrosion of the metal. In the cast-iron container, the formic acid and peroxide reacted with the metal to form iron formate. Analysis of the corrosion product indicated that its empirical formula was $FeO(HCOO) \cdot H_2O$.

The corrosion tendencies of neat alcohols decreased with increasing molecular weight. Neat methanol combustion residues caused significant corrosion of cast iron, while those from neat isopropanol formed negligible corrosion product. Correspondingly, the amount of combustion residue formed decreased rapidly as the molecular weight of the alcohol was increased. Hydrocarbons such as isooctane formed neither combustion residues nor corrosion products.

Alcohol/water blends caused significantly more corrosion than neat alcohols. For example, isopropanol with 10 percent water caused substantial corrosion of the cast-iron container. The quantities of formaldehyde and formic acid in residues from alcohol/water blends decreased rapidly as the molecular weight of the alcohol was increased, but the amounts of peroxide remained about the same. The decrease in the concentrations of formaldehyde and formic acid with increasing molecular weight of the alcohol was caused by (1) differences in chemistry and (2) the relative volatilities of the formaldehyde and formic acid compared to the peroxide, and (3) the increased tendency for residue evaporation as the boiling point of the alcohol increased.

Concentration-time profiles of combustion products dissolved in burning pools of methanol and ethanol showed that the relative volatilities of the products decreased in the order, water > formaldehyde > formic acid > peroxide. The conclusion is that the relatively low volatilities of formic acid and peroxide would cause them to concentrate as combustion residues evaporate from surfaces such as a cylinder wall.

Measurements of relative rates of iron dissolution by various synthetic residue compositions showed that electrolytic corrosion attributed to formic acid was significantly enhanced by the peroxide. The conclusion is that the peroxide causes significant oxidation of iron and thus must play an important role in the corrosion process.

The kinetics of formic acid formation (see Appendix) from the reaction of hydrogen peroxide with formaldehyde was examined because this reaction appears to be important in the mechanism of formic acid formation in the low-temperature combustion of alcohols. It was found that one mole of hydrogen peroxide reacted with two moles of formaldehyde to form one mole of dioxy-methylene peroxide, which decomposed into two moles of formic acid and one mole of hydrogen. A kinetic model was developed to ascertain the unimolecular rate constant for the decomposition of dioxymethylene peroxide and the equilibrium constant that relates the concentrations of dioxymethylene peroxide, hydrogen peroxide, and formaldehyde. Based on the kinetic model, it was found that the equilibrium constant for the reaction

69

$$H_2O_2 + 2HCHO \rightleftharpoons (CH_2OH)-OO-(CH_2OH)$$
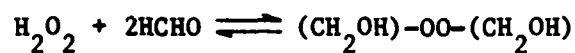
was 66.6 liters^2/moles^2 and the unimolecular rate constant for the reaction

$$(CH_2OH)_2O_2 = 2HCOOH + H_2$$

was 2.56×10^{-6} sec^{-1} at a temperature of 23°C.

Based on this preliminary kinetics study, the conclusion is that dioxymethylene peroxide is the peroxide which is present in combustion residues of low molecular weight alcohols. It also appears that dioxymethylene peroxide is the precursor to the formation of formic acid in the low-temperature combustion of alcohols.

VI. REFERENCES

1. Owens, E.C., Marbach, H.W., Jr., Frame, E.A., and Ryan, T.W., III, "Effects of Alcohol Fuels on Engine Wear," Interim Report AFLRL No. 133, AD A098258, Contract No. DAAK70-79-C-0175, prepared by U.S. Army Fuels and Lubricants Research Laboratory, October 1980 ; SAE Paper No. 800857.

2. Marbach, H.W., Jr., Owens, E.C., Ryan, T.W., III, Frame, E.A., and Naegeli, D.W., "Evaluation of the Effects of Alcohol Fuels on Spark Ignition Engine Wear," Final Report AFLRL No. 150, AD A110021, Contract No. DAAK70-79-C-0175, prepared by U.S. Army Fuels and Lubricants Laboratory, December 1981.

3. Marbach, H.W., Jr., Frame, E.A., Owens, E.C., and Naegeli, D.W., "The Effects of Alcohol Fuels and Fully Formulated Lubricants on Engine Wear," SAE Paper No. 811199, 1981.

4. Marbach, H.W., Jr., Frame, E.A., Owens, E.C., and Naegeli, D.W., "The Effects of Lubricant Composition on S.I. Engine Wear With Alcohol Fuels," SAE Paper No. 831702, 1983.

5. Naman, T.W. and Striegler, B.C., "Engine and Field Test Evaluation of Methanol as an Automotive Fuel," SAE Paper No. 831703, 1983.

6. King, E.T. and Chui, D.K, "Hardware Effects on the Wear of Methanol Fueled Engines," 6th International Symposium on Alcohol Fuels Technology, Paper A-36, Vol. 1, p. 242, May 1984.

7. Ogston, A.R., "Alcohol Motor Fuels," Journal of the Institute of Petroleum Technologies, August 1937.

8. Egloff, G. and Morrell, J.R., "Alcohol-Gasoline as Motor Fuel," Industrial and Engineering Chemistry, Vol. 28, No. 9, p. 1080, September 1936.

9. Eyzat, P., "Utilization of Methanol in Engines With Controlled Ignition," Revue de l'Association Francaise des Technicians du Petrole, pp. 31-35, 1974.

10. Miller, E., Continental Oil Company, Personal Communications with Mr. E. C. Owens, 1977.

11. Owens, E.C., "Methanol-Fuel Effects on Spark Ignition Lubrication and Wear," International Symposium on Alcohol Fuel Technology-Methanol and Ethanol, Wolfsburg, Germany, November 1977.

12. Brady, D.C., Franklin, T.M., and Roberts, C.E., "A 2.3L Engine Deposit and Wear Test--An ASTM Task Force Progress Report," SAE Preprint No. 780260, February 1978.

13. Chui, G.K. and Millard, D.H.T., "Development and Testing of Crankcase Lubricants for Alcohol-Fueled Engines," SAE Paper No. 811203, October 1981.

14. Chui, G.K., King, E.T., and Pedrys, F., "Evaluation of Lubricants for Methanol-Fueled Engines," The Proceedings of the Fifth Symposium on Alcohol Fuel Technology, Auckland, New Zealand, May 1982.

15. Chaibongsai, S., Howlett, B.J., and Millard, D.H.T., "Development of an Engine Screening Test to Study the Effects of Methanol Fuel on Crankcase Oils," SAE Paper No. 830240, February 1983.

16. Marbach, H.W., Jr., Owens, E.C., and Frame, E.A., "Technical Support for Resolving Wear Problems in Alcohol-Fueled Engines," Report No. SwRI-7152/1, March 1983.

17. Owens, E.C., Marbach, H.W., Jr., Frame, E.A., and Ryan, T.W., III, "Effects of Alcohol Fuels on Engine Wear," SAE Paper No. 800857, 1980.

18. Quillian, R.D., et al., "Cleaner Crankcases With Blowby Diversion," SAE Paper No. 801B, January 1964.

19. Ernst, R.J., Pefley, R.K., and Wiens, F.J., "Methanol Engine Durability," SAE Paper No. 831704, 1983.

20. Naegeli, D.W., Yost, D.M., and Owens, E.C., "Engine Wear with Methanol Fuel in a Nitrogen-Free Environment," SAE Paper No. 841374, 1984.

21. Spalding, D.B., "Some Fundamentals of Combustion," Gas Turbine Series Vol. 2, p. 59, Butterworths Scientific Publications, London, 1955.

22. Otto, K., Bartosiewicz, L., and Carter, R.O., III, "Steel Corrosion by Methanol Combustion Products," Paper has been submitted for publication in "Corrosion Science," 1984.

23. Seshadri, K., "Structure and Extinction of Laminar Diffusion Flames Above Condensed Fuels With Water and Nitrogen," Combustion and Flame, Vol. 33, No. 197, 1978.

24. Aronowitz, D., Naegeli, D.W., and Glassman, I., "The High-Temperature Pyrolysis of Methanol," J. Phys. Chem., Vol. 81, pp. 2555, 1977.

25. Aronowitz, D., Santoro, R.J., Dryer, F.L., and Glassman, I., "Kinetics of the Oxidation of Methanol: Experimental Results Semi-Global Modeling and Mechanistic Concepts," 17th Symposium (International) on Combustion, p. 633, 1978.

26. Bricker, C.E. and Johnson, H.R., "Spectrometric Method for Determining Formaldehyde," Industrial and Engineering Chemistry (Analytical Edition) Vol. 17, p. 400, 1945.

27. Egerton, A.C., Everett, A.J., Minkoff, G.J., Rudrakanchana, S., and Salooja, K.C., "The Analysis of Combustion Products: I. Some Improvements in the Methods of Analysis of Peroxides," Analytica Chimica Acta, Vol. 10, p. 422, 1954.

28. Jupille, T., Burge, D., and Togami, D., "Ion Chromatography Uses Only One Column to Get All the Ions," Research and Development, p. 135, March 1984.

29. Ryan, T.W., III, Naegeli, D.W., Owens, E.C., Marbach, H.W., Jr., and Barbee, J.G., "The Mechanism Leading to Increased Cylinder Bore and Ring Wear in Methanol-Fueled S.I. Engines," SAE Paper No. 811200, Tulsa, OK, 19-22 October 1981.

30. Mack, E., Jr., Garrett, A.B. Haskins, J.F., and Verback, F.H., "Textbook of Chemistry," 2nd Edition, Ginn and Company, New York and London, p. 227, 1956.

31. Scully, J.C., "The Fundamentals of Corrosion," Pergamon Press, Oxford, London, New York, Toronto, Paris, and Frankfurt, p. 49, 1966.

APPENDIX

KINETICS OF FORMIC ACID FORMATION
IN THE COMBUSTION OF ALCOHOLS

KINETICS OF FORMIC ACID FORMATION
IN THE COMBUSTION OF ALCOHOLS

Throughout the history of combustion chemistry, several stable intermediates and free radical species have been discovered. Lewis and von Elbe (1)* give some mention of formic acid, but, for the most part, it has been ignored in the combustion chemistry of alcohols and hydrocarbons. As of late, the presence of formic acid in combustion gases and liquid condensates has become more important because of the role that it appears to play in the corrosion of rings and cylinder bores of methanol-fueled spark ignition engines.

In reviewing the literature, it is apparent that the mechanism for the formation of formic acid in the combustion of alcohols and hydrocarbons is not well known. About four decades ago, Bone and Gardner (2) and Style and Summers (3) studied the slow gas phase oxidation chemistry of methane, methanol, and formaldehyde at temperatures in the range of 100° to 300°C. This temperature range is of particular interest because it is what one might expect to find near the surface of burning liquid pools. In their studies of the low temperature oxidation of formaldehyde, they found several combustion intermediates including formic acid, performic acid, and what appeared to be dioxymethylene peroxide. These intermediates were also observed in the low temperature oxidation of methanol, and it was apparent that their formation rates were proportional to the concentration of formaldehyde which is formed as an intermediate in pyrolysis (4) and oxidation (5) of methanol. The results of the formaldehyde oxidation work (2,3) indicated that dioxymethylene peroxide, $CH_2OH - OO - CH_2OH$, was a precursor to the formation of formic

---

* Underscored numbers in parentheses refer to the references at the end of this appendix.

acid and performic acid. Dioxymethylene peroxide can be formed by the reaction of hydrogen peroxide with formaldehyde as follows

$$H_2O_2 + 2HCHO = \overset{\overset{\displaystyle OH}{|}}{CH_2} - OO - \overset{\overset{\displaystyle OH}{|}}{CH_2}$$
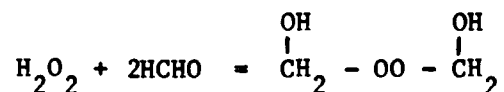
and it is believed to decompose via

$$\overset{\overset{\displaystyle OH}{|}}{CH_2} - OO - \overset{\overset{\displaystyle OH}{|}}{CH_2} = 2HCOOH + H_2$$
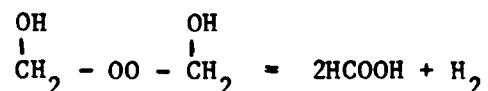
forming hydrogen and two moles of formic acid. The mechanism for the formation of dioxymethylene peroxide in the combustion of methanol and formaldehyde is not known, but it is very possible that the species involved are hydrogen peroxide and formaldehyde. It is well known ($\underline{1},\underline{5}$) that hydrogen peroxide is formed as an intermediate in the combustion of alcohols and hydrocarbons. It is formed most readily in oxidations of methanol and formaldehyde because free radical reactions such as

$$CH_2OH + O_2 = HCHO \quad HO_2$$

and

$$HCO + O_2 = CO + HO_2$$

followed by

$$HO_2 + RH = H_2O_2 + R$$

occur very frequently. Formic acid is not observed in the high temperature oxidations of methanol and formaldehyde.($\underline{5}$) This may well be due to the fact

that peroxides are relatively unstable at temperatures greater than 500K. If the concentration of hydrogen peroxide is very low because of unimolecular decomposition via

$$H_2O_2 = 2OH$$

it would not have the opportunity to react with two moles of formaldehyde to form dioxymethylene peroxide which is also expected to be very unstable at high temperatures. This appears to be the reason why formic acid is only found in low temperature combustion, i.e., in regions of flame quench such as the gaseous boundary layer of a cylinder wall.

Recent work by Sarkissian and Malkhassian (6) on the mass spectrometric analysis of the oxidation products of formaldehyde showed that several intermediates including formic acid and hydrogen peroxide were formed, but performic acid and dioxymethylene peroxide were not detected. If dioxymethylene peroxide had been an important intermediate in the formation of formic acid, its steady-state concentration must have been very low. The oxidation experiments were carried out at temperatures ranging from 350° to 500°C. At these temperatures, dioxymethylene peroxide probably decomposes immediately upon formation.

The kinetics of the reaction of hydrogen peroxide with formaldehyde in the aqueous phase was recently studied by Baranchik, et al. (7) in the temperature range of 20° to 60°C. They concluded that hydrogen peroxide disappears via

$$2H_2O_2 = O_2 + 2H_2O$$

and

$$H_2O_2 + HCHO = HCOOH + H_2O$$
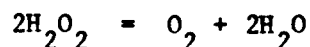
forming a small amount of oxygen and formic acid as the main product. The decomposition of hydrogen peroxide in the first reaction is relatively slow compared to the bimolecular reaction with formaldehyde. This mechanism put forth by Baranchik, et al. assumes that one mole of formic acid is formed from one mole of hydrogen peroxide, and there is no evidence given in their paper for the formation of a dioxymethylene peroxide intermediate. If dioxy-methylene peroxide was actually formed in the aqueous phase from hydrogen peroxide and formaldehyde as indicated by Fenton (8) several decades ago, its decomposition would no doubt lead to the formation of two moles of formic acid for each mole of hydrogen peroxide consumed.

In order to resolve the differences in the mechanisms reported in the literature, a preliminary investigation of the kinetics of the reaction of hydrogen peroxide with formaldehyde was made. The purpose of this investigation was to gain a better understanding of the mechanism of formic acid and the structure of the peroxide found in combustion residues.

The kinetics of the reaction were determined by measuring the changes in concentrations of hydrogen peroxide and formic acid in aqueous solutions containing 0.1 percent hydrogen peroxide in 0.0, 0.5, 1.0, and 1.5 percent formaldehyde at a temperature of 23°C. The measurements showed that for every mole of hydrogen peroxide consumed, two moles of formic acid were

formed. This occurred consistently when the reaction was carried out in different reaction vessels, glass and Teflon®, and different initial concentrations of formaldehyde. It was also found that hydrogen containing a trace (<1 percent) of oxygen was evolved in the reaction. At higher temperatures (ca. 40°C), the gas contained a small amount (ca. 1 percent) of carbon dioxide which may have been formed from the decomposition of performic acid or possibly formaldehyde peroxide, $CH_2OH - OOH$. The evolution of hydrogen seemed to indicate that hydrogen atoms might be important in the mechanism since they are expected to react with formaldehyde as shown below:

$$H + HCHO = H_2 + HCO \tag{A-1}$$

However, if hydrogen was formed by H atom abstraction, the resulting formyl radicals should have combined, as shown below, to form carbon monoxide and hydrogen.

$$HCO + HCO = H_2 + 2CO \tag{A-2}$$

Since carbon monoxide was not found in the gaseous products, it appears that hydrogen atoms were not formed, and it suggests that both hydrogen and formic acid were formed in one step.

The rate of disappearance of peroxide was found to be a first order process. This is shown in Figure A-1 where the natural logarithm of the peroxide concentration is plotted versus time. The curves are shown for the decomposition of peroxide in pure water and in water containing 0.5, 1.0, and 1.5 percent formaldehyde. The slopes of the curves represent "global" rate constants for the disappearance of peroxide. The rate constants are termed

"global" because they change with the concentration of formaldehyde and thus must be a function of the formaldehyde concentration. Figure A-2 shows that the "global" rate constants for the disappearance of peroxide are a complex function of the formaldehyde concentration. It is clear from the coordinates of the points that the reaction is not simply first or second order in the formaldehyde concentration. If that was so, the points would fall on a straight line passing through the origin. The complex dependence indicated by the theoretical curve in Figure A-2 is based on the assumption that formic acid is formed from the decomposition of dioxymethylene peroxide. The over-all reaction is assumed to be

$$H_2O_2 + 2HCHO \underset{K_{-1}}{\overset{K_1}{\rightleftharpoons}} \quad H-\overset{\overset{\textstyle H}{|}}{\underset{\underset{\textstyle OH}{|}}{C}}-O-O-\overset{\overset{\textstyle H}{|}}{\underset{\underset{\textstyle OH}{|}}{C}}-H \quad \overset{K_2}{=} \quad 2HCOOH + H_2$$
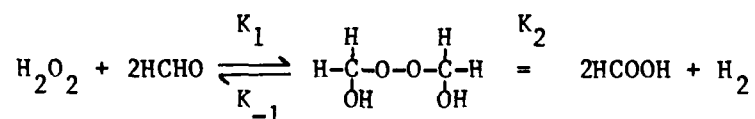
where hydrogen peroxide and formaldehyde are in equilibrium with dioxymethylene peroxide; K_1 and K_{-1} are the forward and backward rate constants and K_2 is the unimolecular rate constant for the decomposition of dioxymethylene peroxide into formic acid and hydrogen.

In order to simplify the nomenclature, the concentrations of hydrogen peroxide, formaldehyde, and dioxymethylene peroxide are expressed as A, B, and C, respectively. A fourth term, P, is used to express the measured peroxide concentration; it is the sum of the hydrogen peroxide and dioxymethylene peroxide concentrations.

$$P = A + C \tag{A-3}$$

82

The equilibrium constant for dioxymethylene peroxide, C, may be expressed as

$$K_{eq} = \frac{K_1}{K_{-1}} = \frac{C}{AB^2} \qquad (A-4)$$

and the rate of disappearance of peroxide, P, may be expressed as

$$- \frac{dP}{dt} = K_2 C \qquad (A-5)$$

It is assumed that the equilibrium between A, B, and C is established rapidly, whereas the rate of decomposition of C is a relatively slow process. In other words, the disappearance of the peroxide, in the form of C, is the rate controlling step. Based on Equations A-3 through A-5, it can be shown that

$$- dlnP/dt = (K_2 B^2)/(K_{eq}^{-1} + B_2) \qquad (A-6)$$

The theoretical curve shown in Figure A-2 is the best curve fit of the data using Equation A-6 and assuming that the "global" rate constant for the peroxide decomposition is 0.18×10^{-6} sec^{-1} when the concentration of formaldehyde is zero. From the best curve fit of the data to Equation A-7,

$$- dlnP/dt = 0.18 \times 10^{-6} + (2.56 \times 10^{-6} B^2)/(0.015 + B^2) \qquad (A-7)$$

it is seen that the unimolecular rate constant $K_2 = 2.56 \times 10^{-6}$ sec^{-1} and the equilibrium constant $K_{eq} = 66.6$ liters^2/mole^2 at 23°C. Based on this value of K_2, the half life of dioxymethylene peroxide is 2.7×10^5 seconds or 3.13 days at 23°C. The equilibrium constant is substantially greater than unity, indicating that dioxymethylene peroxide is relatively more stable than the

reactants, hydrogen peroxide and formaldehyde. The results show that combustion residues must contain dioxymethylene peroxide, instead of hydrogen peroxide.

The rate of dioxymethylene peroxide decomposition into formic acid is expected to increase quite dramatically with temperature. It was not possible to estimate the activation energy of the reaction from experimental data, because the reaction rate was only measured at 23°C. However, the activation energy may be estimated from the strength of the O-O bond in the peroxide group.

Peroxidic O-O bond energies are generally in the range of about 40 to 45 kcal/mole. Assuming that the activation energy is in this range, the half life of dioxymethylene peroxide at 100°C could be as brief as 0.4 seconds. If it forms in relatively cool boundary layers, quench zones, etc., it could easily account for the formic acid that is found in combustion residues of methanol. The dioxymethylene peroxide found in combustion residues probably forms from hydrogen peroxide and formaldehyde that diffuse from the flame zone and dissolve in the liquid medium before reaction is possible in the gas phase.
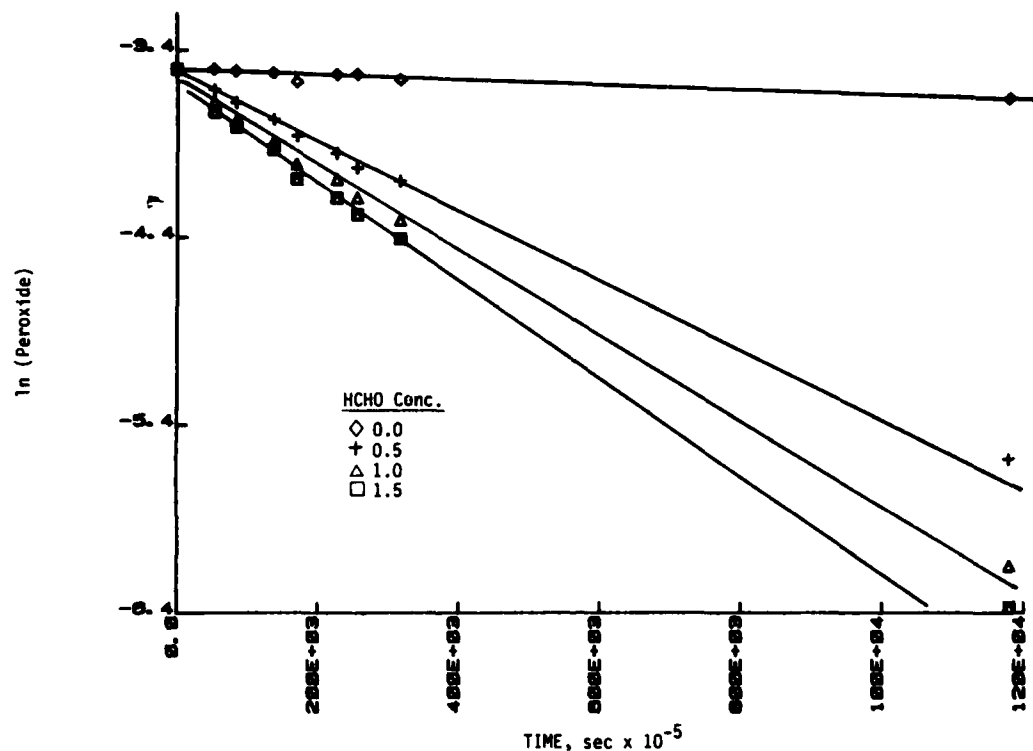
FIGURE A-1. FIRST ORDER DECAY OF PEROXIDE CONCENTRA-
TION IN AQUEOUS SOLUTIONS OF FORMALDEHYDE

$$- \frac{d\ln P}{dt} = 0.183 \times 10^{-6} + \frac{2.56 \times 10^{-6} \, B^2}{0.015 + B^2}$$
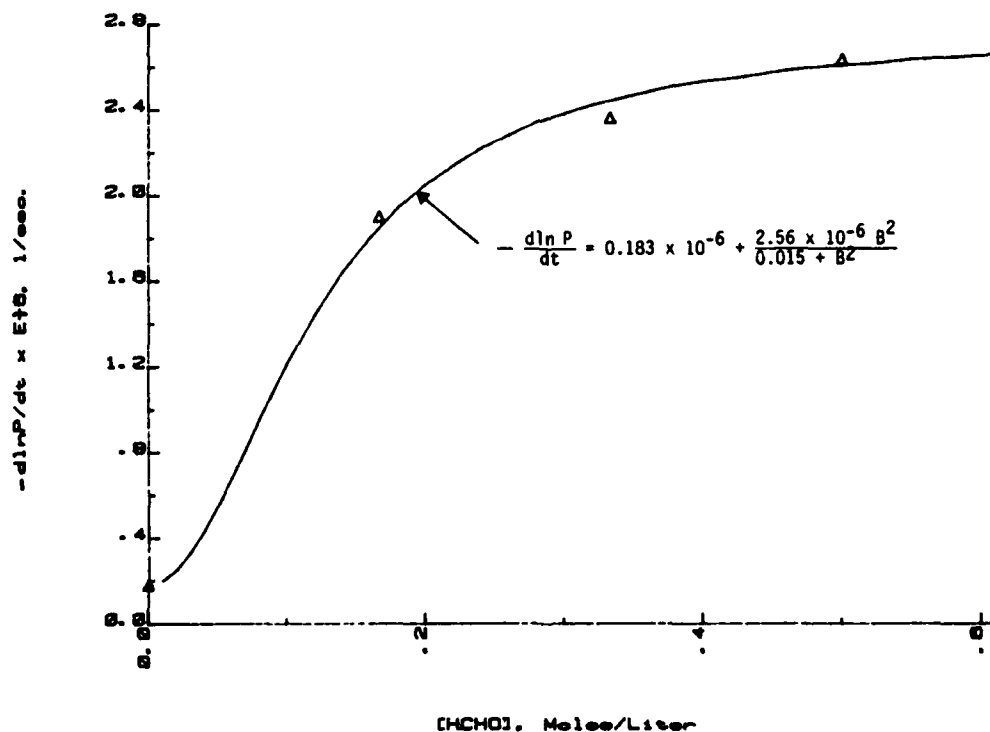
FIGURE A-2. EFFECT OF FORMALDEHYDE CONCENTRATION ON THE
"GLOBAL" FIRST ORDER RATE OF DECAY OF PEROXIDE
(Theoretical Curve is Best Fit to Data)

85

REFERENCES

1. Lewis, B. and von Elbe, G., "Combustion, Flames and Explosions of Gases," 2nd Ed., p. 93, Academic Press, Inc., New York and London (1961).

2. Bone, W.A. and Gardner, J.B., "Comparative Studies of the Slow Combustion of Methane, Methyl Alcohol, Formaldehyde, and Formic Acid," Proc. Roy. Soc. (London) A154, 297 (1936).

3. Style, D.W.G. and Summers, D., "Photochemical Reaction Between Formaldehyde and Oxygen," Trans. Faraday Soc. 42, 388 (1946).

4. Aronowitz, D., Naegeli, D.W., and Glassman, I., "The High-Temperature Pyrolysis of Methanol," J. Phys. Chem., 81, 2555 (1977).

5. Aronowitz, D., Santors, R.J., Dryer, F.L., and Glassman, I., "Kinetics of the Oxidation of Methanol: Experimental Results Semi-Global Modeling and Mechanistic Concepts," 17th Symposium (International) on Combustion, p. 633 (1978).

6. Sarkissian, E.G., and Malkhassian, R.T., "A Detailed Mass-Spectrometric Analysis of the Oxidation Products of Formaldehyde and Mass-Spectrum of Performic Acid," Arm. Khim. Zh. 31(1), 76-80 (1978).

7. Baranchik, G.N., Zhigunov, I.S., Koroleva, G.N., and Petryaev, E.P., Vestsi Akad. Navuk Belarus, SSR, Ser. Khim. Navuk, 1, 119 (1970).

8. Fenton, A., "Formaldehyde Peroxide," Proc. Roy. Soc., 90A, 492 (1914).

DISTRIBUTION LIST

DEPARTMENT OF DEFENSE

DEFENSE DOCUMENTATION CTR
CAMERON STATION   12
ALEXANDRIA VA   22314

DEPT. OF DEFENSE
ATTN: DASD-LMM (MR DYCKMAN)   1
WASHINGTON DC 20301

CDR
DEFENSE FUEL SUPPLY CTR
ATTN: DFSC-T (MR. MARTIN)   1
CAMERON STA
ALEXANDRIA VA   22314

CDR
DEFENSE GENERAL SUPPLY CTR
ATTN: DGSC-SSA (MR MENCHARINI)   1
       DGSC-STC (MR DOYLE)   1
RICHMOND VA   23297

DOD
ATTN: DUSDRE (RAT) (Dr. Dix)   1
       ROOM 3-D-1089, PENTAGON   1
WASHINGTON DC 20301

DEFENSE ADVANCED RES PROJ AGENCY
DEFENSE SCIENCES OFC   1
1400 WILSON BLVD
ARLINGTON VA   22209

DEPARTMENT OF THE ARMY

HG, DEPT OF ARMY
ATTN: DALO-TSE (COL NAJERA)   1
       DALO-AV   1
       DALO-SMZ-E   1
       DAMA-ARZ-E (DR CHURCH)   1
       DAMA-ART (LTC RINEHART)   1
WASHINGTON DC 20310

CDR
U.S. ARMY BELVOIR RESEARCH AND
  DEVELOPMENT CENTER
ATTN: STRBE-VF   10
       STRBE-WC   2
FORT BELVOIR VA   22060

CDR
US ARMY MATERIEL DEVEL &
  READINESS COMMAND
ATTN: AMCLD (DR GONANO)   1
       AMCDE-SG   1
       AMCDRA-ST (DR HALEY)   1
       AMCDE-SS   1
       AMCQA-E   1
       AMCQA-P (MR TINER)   1
       AMCIP-P (MR HARVEY)   1
5001 EISENHOWER AVE
ALEXANDRIA VA 22333

CDR
US ARMY TANK-AUTOMOTIVE CMD
ATTN: AMSTA-RG   1
       AMSTA-ZS (MR REES)   1
       AMSTA-G   1
       AMSTA-MTC (MR GAGLIO),
         AMSTA-MC   1
       AMSTA-GBP (MR MCCARTNEY)   1
       AMSTA-RC   1
       AMSTA-MLF (MR KELLER)   1
WARREN MI 48090

DIRECTOR
US ARMY MATERIEL SYSTEMS
  ANALYSIS AGENCY
ATTN: AMXSY-CM (MR NIEMEYER)   1
       AMXSY-CR   1
ABERDEEN PROVING GROUND MD   21005

DIRECTOR
APPLIED TECHNOLOGY LAB
U.S. ARMY R&T LAB (AVRADCOM)
ATTN: SAVDL-ATL-ATP (MR MORROW) 1
       SAVDL-ATL-ASV   1
FORT EUSTIS VA 23604

CDR
US READINESS COMMAND
ATTN: J4-E   1
MACDILL AIR FORCE BASE FL   33608

DIRECTOR
US ARMY MATERIEL CMD
MATERIEL SUPPORT ACTIVITY
ATTN: AMXTB-T (MR STOLARICK)   1
FORT LEWIS WA   98433

HQ, 172D INFANTRY BRIGADE (ALASKA)
ATTN: AFZT-DI-L   1
       AFZT-DI-M   1
DIRECTORATE OF INDUSTRIAL
 OPERATIONS
FORT RICHARDSON AK 99505

CDR
US ARMY GENERAL MATERIAL &
  PETROLEUM ACTIVITY
ATTN: STSGP-F (MR ASHBROOK)   1
      STSGP-PE, BLDG 85-3   1
      STSGP-G (COL CLIFTON)   1
NEW CUMBERLAND ARMY DEPOT
NEW CUMBERLAND PA 17070

CDR
US ARMY MATERIEL ARMAMENT
       READINESS CMD
ATTN: AMSAR-LEM   1
ROCK ISLAND ARSENAL IL 61299

CDR
US ARMY COLD REGION TEST CENTER
ATTN: STECR-TA   1
APO SEATTLE 98733

HQ, DEPT. OF ARMY
ATTN: DAEN-DRM   1
WASHINGTON DC   20310

CDR
US ARMY RES & STDZN GROUP
  (EUROPE)
ATTN: AMXSN-UK-RA   1
      AMXSN-UK-SE (LTC NICHOLS)   1
BOX 65
FPO NEW YORK 09510

HQ, US ARMY AVIATION R&D CMD
ATTN: AMSAV-EP (MR EDWARDS)   1
      AMSAV-NS   1
4300 GOODFELLOW BLVD
ST LOUIS MO 63120

CDR
US ARMY FORCES COMMAND
ATTN: AFLG-REG   1
      AFLG-POP   1
FORT MCPHERSON GA 30330

CDR
US ARMY BALLISTIC RESEARCH LAB
ATTN: AMXBR-VLD (MR ARMENDT)   1
      AMXBR-LBD (DR MENNE)   1
ABERDEEN PROVING GROUND MD   21005

CDR
US CENTRAL COMMAND
ATTN: CINCCEN/CC J4-L   1
MACDILL AIR FORCE BASE FL   33608

CDR
US ARMY ABERDEEN PROVING GROUND
ATTN: STEAP-MT-U (MR DEAVER)   1
ABERDEEN PROVING GROUND MD   21005

CDR
US ARMY YUMA PROVING GROUND
ATTN: STEYP-MLS-M (MR DOEBBLER)   1
YUMA AZ 85364

PROJ MGR, BRADELY FIGHTING
  VEHICLE SYS
ATTN: AMCPM-FVS-M   1
WARREN MI 48090

PROG MGR, M113/M113A1 FAMILY
  VEHICLES
ATTN: AMCPM-M113-T   1
WARREN MI 48090

PROJ MGR, MOBILE ELECTRIC POWER
ATTN: CPM-MEP-TM   1
7500 BACKLICK ROAD
SPRINGFIELD VA 22150

PROJ OFF, AMPHIBIOUS AND WATER
  CRAFT
ATTN: AMCOP-AWC-R   1
4300 GOODFELLOW BLVD
ST LOUIS MO 63120

CDR
US ARMY EUROPE & SEVENTH ARMY
ATTN: AEAGG-FMD   1
      AEAGD-TE   1
APO NY 09403

CDR
THEATER ARMY MATERIAL MGMT
  CENTER (200TH)
DIRECTORATE FOR PETROL MGMT
ATTN: AEAGD-MMC-PT-Q   1
APO NY 09052

CDR
US ARMY RESEARCH OFC
ATTN: AMXRO-ZC   1
        AMXRO-EG (DR MANN)   1
        AMXRO-CB (DR GHIRARDELLI) 1
P O BOX 12211
RSCH TRIANGLE PARK NC 27709

PROG MGR, TACTICAL VEHICLE
ATTN: AMCPM-TV   1
WARREN MI   48090

DIR
US ARMY AVIATION R&T LAB (AVRADCOM)
ATTN: SAVDL-AS (MR WILSTEAD)   1
NASA/AMES RSCH CTR
MAIL STP 207-5
MOFFIT FIELD CA   94035

CDR
TRADOC COMBINED ARMS TEST
  ACTIVITY
ATTN: ATCT-CA   1
FORT HOOD TX 76544

CDR
105TH S & T BATTALION
ATTN: LTC MCLEMORE   1
5TH INFANTRY DIV (MECH)
FORT POLK LA 71459

CDR
TOBYHANNA ARMY DEPOT
ATTN: SDSTO-TP-S   1
TOBYHANNA PA 18466

CDR
US ARMY DEPOT SYSTEMS CMD
ATTN: AMSDS   1
CHAMBERSBURG PA 17201

CDR
US ARMY WATERVLIET ARSENAL
ATTN: SARWY-RDD   1
WATERVLIET NY 12189

CDR
US ARMY LEA
ATTN: DALO-LEP   1
NEW CUMBERLAND ARMY DEPOT
NEW CUMBERLAND PA 17070

CDR
US ARMY GENERAL MATERIAL &
  PETROLEUM ACTIVITY
ATTN: STSGP-PW (MR PRICE)   1
BLDG 247, DEFENSE DEPOT TRACY
TRACY CA   95376

PROJ MGR, LIGHT ARMORED VEHICLES
ATTN: AMCPM-LA-E   1
WARREN MI   48090

CDR
US ARMY ORDNANCE CENTER & SCHOOL
ATTN: ATSL-CD-CS   1
ABERDEEN PROVING GROUND MD   21005

CDR
US ARMY FOREIGN SCIENCE & TECH
  CENTER
ATTN: AMXST-MT-1   1
        AMXST-BA   1
FEDERAL BLDG
CHARLOTTESVILLE VA   22901

CDR
US ARMY MATERIEL CMD
MATERIEL READINESS
  SUPPORT ACTIVITY (MRSA)
ATTN: AMXMD-MO (MR BROWN)   1
LEXINGTON KY   40511

HQ, US ARMY T&E COMMAND
ATTN: AMSTE-TO-O   1
        AMSTE-CM-R-O   1
ABERDEEN PROVING GROUND MD   21005

CDR, US ARMY ARMAMENT MUNITIONS &
  CHEMICAL COMMAND
ARMAMENT RESEARCH & DEVELOPMENT CTR
ATTN: AMSMC-LC   1
        AMSMC-SC   1
DOVER NJ   07801

CDR, US ARMY TROOP SUPPORT COMMAND
ATTN: AMST-ME   1
        AMST-WJ (LTC FOSTER)   1
        AMST-S (COL WILBUR)   1
4300 GOODFELLOW BLVD
ST LOUIS MO   63120

DEPARTMENT OF THE ARMY
CONSTRUCTION ENG RSCH LAB
ATTN: CERL-EM   1
        CERL-ZT⌐   1
        CERL-EH   1
P O BOX 4005
CHAMPAIGN IL 61820

TRADOC LIAISON OFFICE
ATTN: ATFE-LO-AV   1
4300 GOODFELLOW BLVD
ST LOUIS MO 63120

CDR
11TH TRANSPORTATION BATTALION
  (TERMINAL)
ATTN: AFFG-I-CDR   1
FORT STORY VA 23459

HQ
US ARMY TRAINING & DOCTRINE CMD
ATTN: ATCD-SL (MAJ JONES)   1
FORT MONROE VA 23651

DIRECTOR
US ARMY RSCH & TECH LAB (AVRADCOM)
PROPULSION LABORATORY
ATTN: SAVDL-PL-D (MR ACURIO)   1
21000 BROOKPARK ROAD
CLEVELAND OH 44135

CDR
US ARMY NATICK RES & DEV LAB
ATTN: STRNA-YE (DR KAPLAN)   1
        STRNA-U   1
NATICK MA 01760

CDR
US ARMY TRANSPORTATION SCHOOL
ATTN: ATSP-CD-MS (MR HARNET)   1
FORT EUSTIS VA 23604

PROJ MGR, PATRIOT PROJ OFFICE
US ARMY MATERIEL CMD
ATTN: AMCPM-MD-T-G   1
REDSTONE ARSENAL AL 35809

CDR
US ARMY QUARTERMASTER SCHOOL
ATTN: ATSM-CD   1
        ATSM-TD   1
        ATSM-PFS   1
FORT LEE VA 23801

HQ, US ARMY ARMOR CENTER AND
  FORT KNOX
ATTN: ATSB-CD   1
FORT KNOX KY 40121

CDR
101ST AIRBORNE DIV (AASLT)
ATTN: AFZB-KE-J   1
        AFSB-KE-DMMC   1
FORT CAMPBELL KY 42223

CDR
US ARMY WESTERN COMMAND
ATTN: APLG-TR   1
FORT SCHAFTER HI 96858

CDR
COMBINED ARMS COMBAT DEVELOPMENT
  ACTIVITY
ATTN: ATZL-CAT-E   1
        ATZL-CAL-A   1
FORT LEAVENWORTH KA 66027

CDR
US ARMY LOGISTICS CTR
ATTN: ATCL-MS (MR A MARSHALL)   1
        ATCL-C   1
FORT LEE VA 23801

CDR
US ARMY FIELD ARTILLERY SCHOOL
ATTN: ATSF-CD   1
FORT SILL OK 73503

CDR
US ARMY ENGINEER SCHOOL
ATTN: ATZA-TSM-C   1
        ATZA-CDM   1
        ATZA-CDD   1
FORT BELVOIR VA 22060-5606

CDR
US ARMY INFANTRY SCHOOL
ATTN: ATSH-CD-MS-M   1
FORT BENNING GA 31905

CDR
MILITARY TRAFFIC MANAGEMENT
  COMMAND
ATTN: MT-SA (MR DOWD)   1
WASHINGTON DC 20315

CDR
US ARMY MISSILE CMD
ATTN: AMSMI-U   1
        AMSMI-RB   1
        AMSMI-S   1
REDSTONE ARSENAL AL 35809

CDR
US ARMY AVIATION CTR & FT RUCKER
ATTN: ATZQ-DI   1
FORT RUCKER AL 36362

PROG MGR, TANK SYSTEMS
ATTN: AMCPM-M1E1   1
        AMCPM-M60   1
WARREN MI 48090

CDR
US ARMY ARMOR & ENGINEER BOARD
ATTN: ATZK-AE-AR   1
        ATZK-AE-LT   1
FORT KNOX KY 40121

CHIEF, U.S. ARMY LOGISTICS
ASSISTANCE OFFICE, FORSCOM
ATTN: AMXLA-FO (MR PITTMAN)   1
FT MCPHERSON GA 30330

CDR
US ARMY SAFETY CENTER
ATTN: PESC-SSD (MR BUCHAN)   1
FORT RUCKER AL 36362

        DEPARTMENT OF THE NAVY

CDR
NAVAL AIR PROPULSION CENTER
ATTN: PE-33 (MR D'ORAZIO)   1
        PE-32 (MR MANGIONE)   1
P O BOX 7176
TRENTON NJ 06828

CDR
NAVAL SEA SYSTEMS CMD
ATTN: CODE 05M4 (MR R LAYNE)   1
WASHINGTON DC 20362

CDR
DAVID TAYLOR NAVAL SHIP R&D CTR
ATTN: CODE 2830 (MR G BOSMAJIAN) 1
        CODE 2705.1 (MR STRUCKO)   1
        CODE 2831   1
ANNAPOLIS MD 21402

CDR
NAVAL SHIP ENGINEERING CENTER
ATTN: CODE 6764 (MR. BOYLE)   1
PHILADELPHIA PA 19112

JOINT OIL ANALYSIS PROGRAM -
    TECHNICAL SUPPORT CTR   1
BLDG 780
NAVAL AIR STATION
PENSACOLA FL 32508

PROJ MGR, M60 TANK DEVELOPMENT
ATTN: USMC-LNO   1
US ARMY TANK-AUTOMOTIVE
    COMMAND (TACOM)
WARREN MI 48090

DEPARTMENT OF THE NAVY
HQ, US MARINE CORPS
ATTN: LPP (MAJ WALLER)   1
        LMM/3 (MAJ WESTERN)   1
WASHINGTON DC 20380

CDR
NAVAL AIR SYSTEMS CMD
ATTN: CODE 5304C1 (MR WEINBURG) 1
        CODE 53645 (MR MEARNS)   1
WASHINGTON DC 20361

CDR
NAVAL AIR DEVELOPMENT CTR
ATTN CODE 60612   1
WARMINSTER PA 18974

CDR
NAVAL RESEARCH LABORATORY
ATTN: CODE 6170   1
        CODE 6180   1
        CODE 6110 (DR HARVEY)   1
WASHINGTON DC 20375

CDR
NAVAL FACILITIES ENGR CTR
ATTN: CODE 1202B (MR R BURRIS) 1
200 STOVWALL ST
ALEXANDRIA VA 22322

CHIEF OF NAVAL RESEARCH
ATTN: CODE 473   1
ARLINGTON VA 22217

CDR
NAVAL AIR ENGR CENTER
ATTN: CODE 92727   1
LAKEHURST NJ 08733

COMMANDING GENERAL
US MARINE CORPS DEVELOPMENT
  & EDUCATION COMMAND
ATTN: DO74 (LTC WOODHEAD)   1
QUANTICO VA 22134

CDR, NAVAL MATERIEL COMMAND
ATTN: MAT-08E (DR A ROBERTS)   1
      MAT-08E (MR ZIEM)   1
CP6, RM 606
WASHINGTON DC 20360

CHIEF OF NAVAL OPERATIONS
ATTN: OP 413   1
WASHINGTON DC 20350

GG
FLEET MARINE FORCE PACIFIC
ATTN: G4 (COL HARMS)   1
CAMP H.M. SMITH HI 96861

CDR
NAVY PETROLEUM OFC
ATTN: CODE 43   1
CAMERON STATION
ALEXANDRIA VA 22314

DEPARTMENT OF THE AIR FORCE

HQ, USAF
ATTN: LEYSF (COL CUSTER)   1
WASHINGTON DC 20330

HQ AIR FORCE SYSTEMS CMD
ATTN: AFSC/DLF (MAJ VONEDA)   1
ANDREWS AFB MD 20334

CDR
US AIR FORCE WRIGHT AERONAUTICAL
  LAB
ATTN: AFWAL/POSF (MR CHURCHILL) 1
       AFWAL/POSL (MR JONES)   1 .
       AFWAL/MLSE (MR MORRIS)   1
WRIGHT-PATTERSON AFB OH 45433

CDR
SAN ANTONIO AIR LOGISTICS
  CTR
ATTN: SAALC/SFT (MR MAKRIS)   1
       SAALC/MMPRR   1
KELLY AIR FORCE BASE TX 78241

CDR
WARNER ROBINS AIR LOGISTIC
  CTR
ATTN WR-ALC/MMTV (MR GRAHAM)   1
ROBINS AFB GA 31098

CDR
USAF 3902 TRANSPORTATION
  SQUADRON
ATTN: LGTVP (MR VAUGHN)   1
OFFUTT AIR FORCE BASE NE 68113

CDR
HQ 3RD USAF
ATTN: LGSF (MR PINZOLA)   1
APO NEW YORK 09127

CDR
DET 29
ATTN: SA-ALC/SFM   1
CAMERON STATION
ALEXANDRIA VA 22314

OTHER GOVERNMENT AGENCIES

NATIONAL AERONAUTICS AND
  SPACE ADMINISTRATION
LEWIS RESEARCH CENTER
  (ATTN: MR PROK)   1
CLEVELAND OH 44135

DEPARTMENT OF TRANSPORTATION
FEDERAL AVIATION ADMINISTRATION
ATTN: AWS-110, MR NUGENT   1
800 INDEPENDENCE AVE, SW
WASHINGTON DC 20591

US DEPARTMENT OF ENERGY
CE-131.2
ATTN: MR ECKLUND   15
FORRESTAL BLDG
1000 INDEPENDENCE AVE, SW
WASHINGTON DC 20585

ENVIRONMENTAL PROTECTION AGENCY   AGENCY FOR INTERNATIONAL DEVELOPMENT
AIR POLLUTION CONTROL   1 ATTN: MR. D. HOOKER   1
2565 PLYMOUTH ROAD   M/SER/EOMS/POM, ROOM 2155A11
ANN ARBOR MI 48105   WASHINGTON DC 20523

END

FILMED

9-85

DTIC